ORGANIC LIGHT EMITTING DIODE, ITS MATERIALS AND APPLICATION

Abstract

The choosing and content of materials utilized in the manufacture of organic light-emitting diodes (OLEDs) significantly influence the efficiency as well as additional features. This part involves a thorough examination of the classification of OLED materials and the diverse range of variants often seen. There are two primary categorizations of OLED materials, largely differentiated by their separate production methodologies: those fabricated using vacuum evaporation and those manufactured through solution- based processes. The encapsulation of polymer nanoparticles is often achieved by vacuum vaporization, while solution- based nanomaterials include the use of polymers, dendrimers, and small molecule compounds. In addition, it is worth noting that OLED materials may be categorized based upon their emission characteristics, namely as fluorescent, phosphorescent, and thermally triggered delayed fluorescent (TADF) materials. These classifications play a crucial role in determining the underlying processes of emission. Furthermore, it is feasible to classify OLED materials based on their individual functionalities inside the device. The activities included in this set of processes are hole injection, hole transport, emission, host materials inside the emissive layer, electron transport, electron injection, and charge blocking. It is important to recognize the significance of the chemical composition of the anode and cathode materials, as this section provides useful insights into their relevance. Moreover, this section delves into the impact of the chemical orientations of biological materials on the operational mechanisms of organic light- emitting diodes (OLEDs).

Keywords: Molecular orientation, material, vacuum evaporation, solution, small molecule, polymer, dendrimer, electrode

Authors

Sunil Kumar Yadav
Research Scholar
Rama University
Uttar Pradesh Kanpur, India.
Sunilex2015@gmail.com

Hari Om Sharan
Professor
Rama University
Uttar Pradesh Kanpur, India.
drsharan.hariom@gmail.com

C. S. Raghuvanshi
Professor
Rama University
Uttar Pradesh Kanpur, India.
drcsraghuvanshi@gmail.com

I. ORGANIC LIGHT-EMITTING DIODE (OLED) TYPES OF MATERIALS

Organic Light-Emitting Diodes (OLEDs) possess the capacity to use a diverse array of chemicals throughout their manufacturing procedure. Figure 2.1 provides a complete representation of the categorization of OLED materials across many classifications. In the context of manufacturing techniques, OLED materials may be classified into two distinct groups: vacuum evaporation type, which employs a dry process, and solution type, which employs a wet process. Figure 2.2 illustrates three distinct categorizations of OLED devices, which are distinguished based on the specific technical approaches used in their manufacturing processes. Hybrid organic light-emitting diodes (OLEDs) consist of a composite structure that combines organic layers produced by a solution-based approach with organic layers created through vacuum evaporation techniques. A study was undertaken by Fukagawa, Tokito, and their research team at NHK Science and Technical Research Laboratories in Japan, focusing on the advancement of white organic light-emitting diodes (OLEDs). The researchers accomplished this by using solution processing methods to fabricate luminescent layers, afterwards subjecting them to a vacuum environment [1].

Organic light-emitting diodes (OLEDs) are composed of a wide array of constituents, including minuscule molecular materials, polymer materials, and dendrimer materials. Each of these materials plays a vital role in the molecular assembly of organic light-emitting diodes (OLEDs). The primary constituent of materials produced by vacuum evaporation mostly consists of small molecules. Nevertheless, prior research has investigated the application of polymer precursors that initiate polymerization following solidification on the underlying surface [2]. Polymers, dendrimers, and small-molecule compounds are often seen in aqueous states, representing distinct categories of materials. The choice of materials for practical OLED systems is dependent on their distinct advantages and optimal functionalities. As seen in Figure 2.1, OLED materials may be classified into many categories, including hole injection materials, hole transport materials, emissive materials, host materials in the emission layer, electron transport materials, electron injection materials, and charge blocking materials. Substances may also be categorized based on their optical properties, such as fluorescence, phosphorescence, or thermally activated delayed fluorescence (TADF).

The composition of electrode materials, namely the anode and cathode components, plays a crucial role in determining the efficiency of an Organic Light-Emitting Diode (OLED). The aforementioned materials facilitate the production of OLED screens via various approaches.

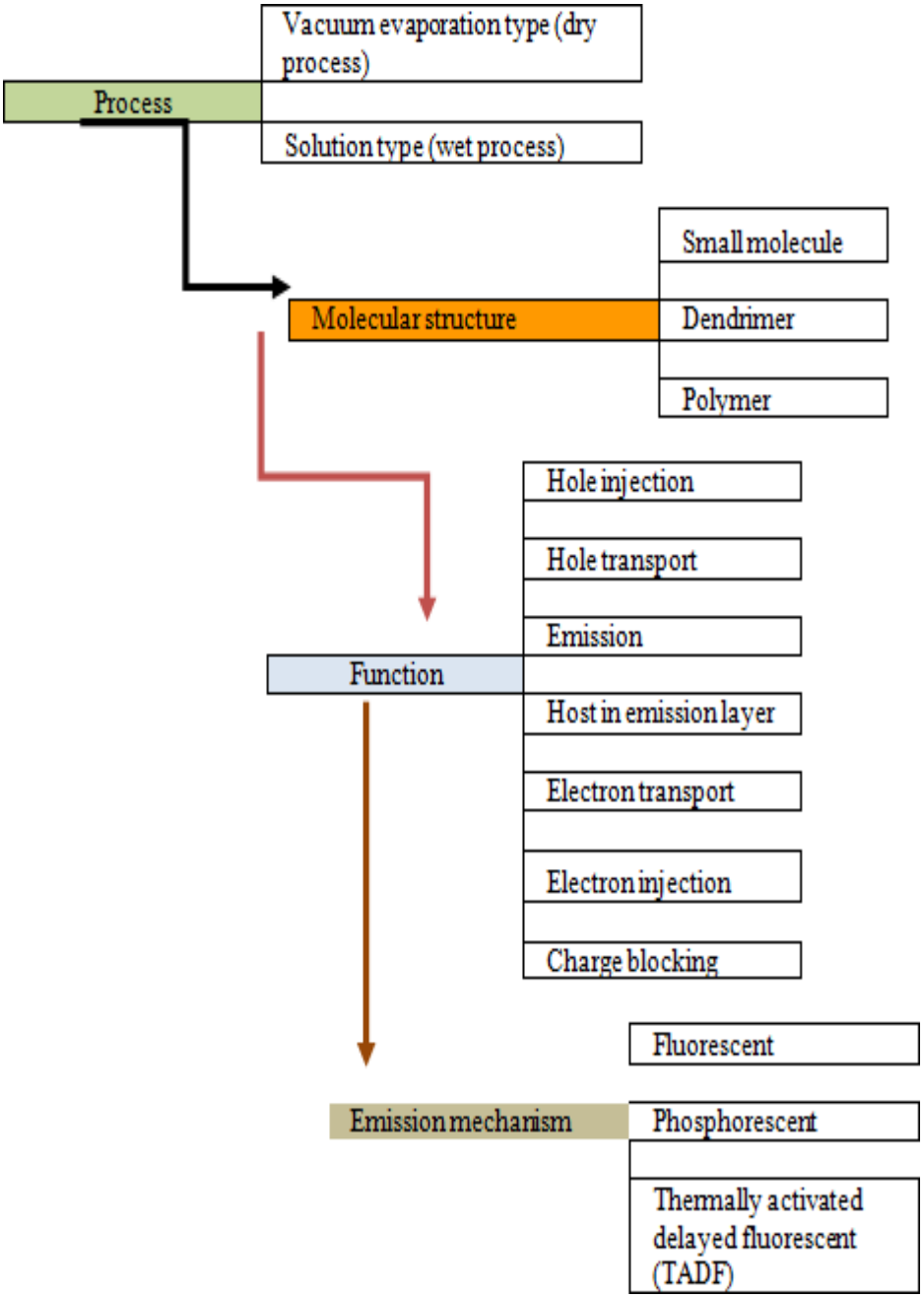

Figure 1: Varieties of Organic Light-Emitting Diode (OLED) Substances

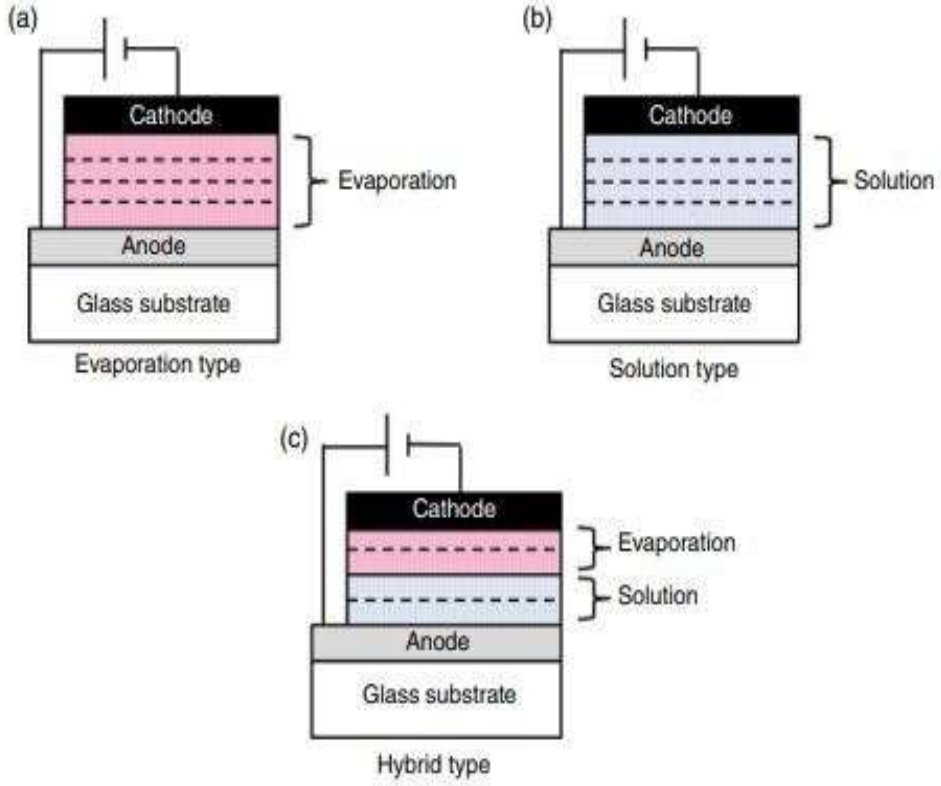

Figure 2: Process-based classifications of three types of OLED devices

II. ANODE MATERIALS

The primary function of the anode is to facilitate the generation of positively charged vacancies, known as holes, within the next layer of naturally occurring energy sources. Given the aforementioned reasons, it is essential that the anode effectively fulfils its designated function. It is of utmost importance for the anode to possess a high work function, considering that the work function of subsequent organic layers, such as a hole injection layer (HIL) or hole transport layer (HTL), typically falls within the range of 5.5 electron volts (eV). Indium tin oxide (ITO) has become the preferred material for the transparent anode in conventional bottom-emission Organic Light-Emitting Diodes (OLEDs), owing to the considerations outlined above.

The deposition procedure is often used to fabricate the ITO layer in a majority of instances. The work function of indium tin oxide (ITO) generally exhibits a range of roughly 4.5 to 5.2 electron volts (eV), with variations influenced by variables such as the specific manufacturing technique used, the properties of the film, and the conditions of the surface. Before applying the second organic layer, it is customary to wash the indium tin oxide (ITO) surface using either O2 plasma [3, 4] or UV-O3 [4, 5] treatment in order to remove any organic residues that may be present on the surface. In addition, it has been shown that these surface treatments have the tendency to elevate the work function, thus enhancing the hole- filling characteristics.

The study conducted by Milliron et al. at Princeton University revealed that the use of oxygen plasma on indium tin oxide (ITO) leads to a notable enhancement in its work function, with an approximate rise of 0.5 electron volts (eV) [3]. The research done by Wu et al. at

Princeton University investigated the effects of O2 plasma therapy and its comparative analysis with other therapeutic interventions for the given medical condition. Furthermore, it has been discovered that there is little modification in the surface contour, suggesting that shape does not play a major role in boosting the performance and stability of the device. The use of UV ozone and oxygen plasma treatments has shown the modification of turn-on voltage and performance. The researchers specifically stated that the use of oxygen plasma treatment produces noteworthy results. Nevertheless, the use of argon (Ar) and hydrogen (H2) plasma therapy did not provide favourable results. The idea proposed that there may be a correlation between changes in the chemical composition of the surface and the effectiveness of hole injection at the interface between ITO and the organic material.

Moreover, a multitude of research and assessments have investigated alternate techniques for surface treatment. Hung et al. (year) did a study at the Eastman Kodak Company to examine the effects of CHF3 on the anode by the use of low-frequency plasma polymerization [6]. The thickness of the polymerized sheet exhibited a range spanning from 2.5 nm to 10 nm. According to their research, the use of this method resulted in greater hole-filling capabilities and improved operational stability. During the first 150 hours of uninterrupted operation at a current density of 40 milliamperes per square centimetre, the OLED device, which was fitted with a polymerized buffer layer measuring 6 nanometers in thickness, exhibited a mere 1% reduction in luminosity. On the other hand, the OLED device without a buffer layer demonstrated a reduction in brightness by 15% over the same time frame.

A further investigation was carried out by Ganzorig et al. under the supervision of Fujihara at the Tokyo Institute of Technology in Japan. This study specifically examined several techniques for surface treatment using benzoyl chlorides, as outlined in their published work [7]. In the present investigation, the scientists used benzoyl chlorides that were ended with H-, Cl-, and CF3- groups for the purpose of surface modification of indium tin oxide (ITO). Subsequently, this changed surface was utilised in the fabrication process of organic light-emitting diode (OLED) devices. The considerable rise in the work function of indium tin oxide (ITO) led to a noteworthy decrease in power consumption. Furthermore, it was noticed that the hierarchy of lowering driving voltage aligned with the hierarchy of rising permanent dipole moments (CF3 > Cl > H).

Self-assembled monolayers (SAMs) are experiencing extensive use across several applications. A research investigation done by Campbell et al. (associated with Los Alamos National Laboratory and The University of Texas at Dallas, USA) shown that the use of self-assembled monolayers (SAM) on an electrode made of metal results in an augmentation of charge injecting. The improved effectiveness could be attributed to the alteration of the Schottky energy barrier between the metallic electrode and an organic material [8].

The ITO material has some drawbacks, including low thermal conductivity, restricted accessibility to rare metals, and a substantial cost. In recent years, there has been a notable surge in the focus on research and development efforts concerning transparent electrodes that do not use indium tin oxide (ITO). The main objective of these initiatives is to explore their possible use in a range of applications, such as OLEDs, touch screens, and related technologies. The primary subject matter of this discourse will revolve on transparent conductive filaments that do not need the use of indium tin oxide (ITO).

In contrast, it should be noted that Organic Light-Emitting Diodes (OLEDs) which emit light from their top surface need the use of a reflective anode. In the case of OLEDs that emit light from the top surface, the anode is often composed of silver (Ag), a combination of silver and indium tin oxide (Ag/ITO), or a stack of indium tin oxide and silver layers (ITO/Ag/Ag/ITO). Silver, often known as Ag, has advantageous characteristics such as a high reflection of visible light and a comparatively low electrical conductivity. The process of cavity filling is greatly impeded due to the relatively high work function of Ag, which is roughly 4.3eV. Hence, the element Ag in isolation is deemed inadequate for the task of hole filling.The use of Ag/ITO stacking seems to be the most optimum strategy. Hsu et al. (Taiwan's National Chiao Tung University and National Tsing Hua University) did a research proposing the use of Ag/ITO stacking as a means to facilitate the development of OLED devices capable of emitting light from the top [9].

In a study done by Chen et al. from National Taiwan University, it was discovered that the implementation of a thin layer of Ag2O, about 10 nm in width, on top of Ag demonstrated successful hole injection. As a result, this phenomenon played a role in enhancing desirable characteristics of organic light-emitting diodes (OLEDs) [10]. Ag2O is categorised as a p-type semiconductor based on its Fermi level, which falls within the range of 4.8 to 5.1 eV. The creation of thin Ag2O was successfully accomplished by the researchers by the utilisation of UV irradiation and ozone treatment, resulting in a significant range of reflectivity spanning from 82% to 91%. The amount of reflection shown by this material is somewhat lower when compared to that of a pristine silver film.

Chong et al. (year) did a study at National Cheng Kung University in Taiwan to examine the impact of tetrahydrofuran (THF), an organic solvent, on a silver anode [11]. The researchers first applied a silver layer over a substrate of indium tin oxide (ITO) coated glass. Following this, the silver anode was submerged in tetrahydrofuran (THF) for a duration of 30 minutes. Following the completion of the reaction, nitrogen gas was used to facilitate the drying process of the tetrahydrofuran (THF)-modified silver (Ag) anode. Subsequently, the desiccated anode was relocated to a glove box that had been purged with nitrogen gas. The use of X-ray photoelectron spectroscopy facilitated an examination that demonstrated the occurrence of chemical bonding between the silver (Ag) surface and THF molecules. This interaction led to the creation of oxygen-rich species through a substrate-catalyzed breakdown mechanism. The work function of silver (Ag) was determined to be 4.79 eV after undergoing treatment with THF, whereas the unaltered silver (Ag) exhibited a work function of 4.54 eV.

A top-emitting organic light-emitting diode (OLED) was fabricated using the following material structure: The structure consists of a layer of indium tin oxide (ITO) and tetrahydrofuran (THF)-modified silver (Ag) on top of a layer of poly(2,5-dimethoxy-1,4-phenylenevinylene) (HY-PPV), followed by a layer of calcium (Ca) with a thickness of 12nm, and finally another layer of silver (Ag) with a thickness of 17nm. In this context, HY- PPV denotes a copolymer derived from poly(para-phenylene-vinylene) that has been subject to modification by the incorporation of phenyl groups. The primary subject matter of this discourse is to the materials used in OLED technology, with particular emphasis on the 29th iteration. The current density of the device under investigation was found to be 2.93cd/A, whereas the current density of the reference device with unaltered Ag exhibited a much lower value of 0.51cd/A. This data implies that the use of THF therapy resulted in a rise in the work function, hence augmenting the current efficiency.

III. VAPORIZE ORGANIC MATERIALS (SMALL MOLECULAR MATERIALS)

In the production process of OLED technological advances, particularly those utilised by applications in industry, a predominant approach involves the utilisation of materials that are evaporated inside a vacuum environment. In general, the materials being examined consist of minuscule molecules that may be classified into several groups according to their individual functionalities. The aforementioned groupings include a range of materials, such as hole injection materials, hole transport materials, releasing materials, host materials in the emission layer, electron transport materials, electron injection materials, and energy obstructing substances, among others as well. In the following part, we shall deliberate about the previously mentioned elements

1. **Hole Injected of OLED Materials:** In the framework of organic light-emitting diodes (OLEDs), there's an observable energy barrier between the anode and the subsequent layer that governs biological functionalities. Hence, it is essential to decrease the magnitude of this obstacle to enable the unhindered movement of charge carriers from the anode to the neighbouring organic layer. Hole injection materials are often used in practical applications of organic light-emitting diode (OLED) devices with the aim of accomplishing this goal. This phenomena may be ascribed to their capacity to decrease the driving voltage, improve efficiency, extend lifetime, and other related factors.

The materials frequently employed for the task of hole topping are shown in Figure 1.3. Materials may be categorised into two distinct groups: biological and artificial. Moreover, some materials have the ability to demonstrate attributes that include elements from both biological and artificial categories, therefore embodying a combination of both features.

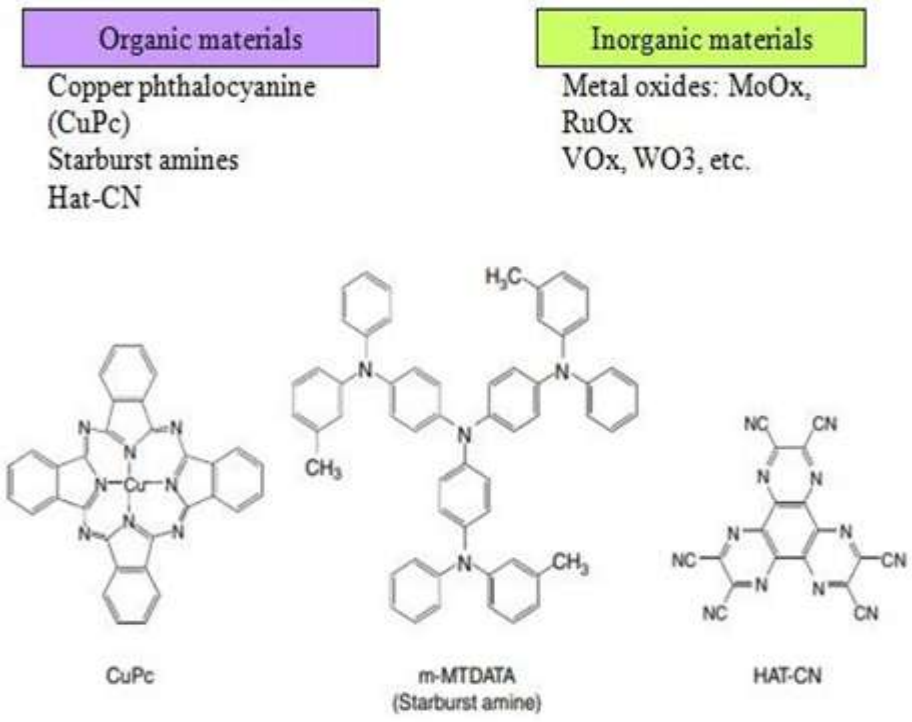

Figure 3: Typical Hole Injection Materials

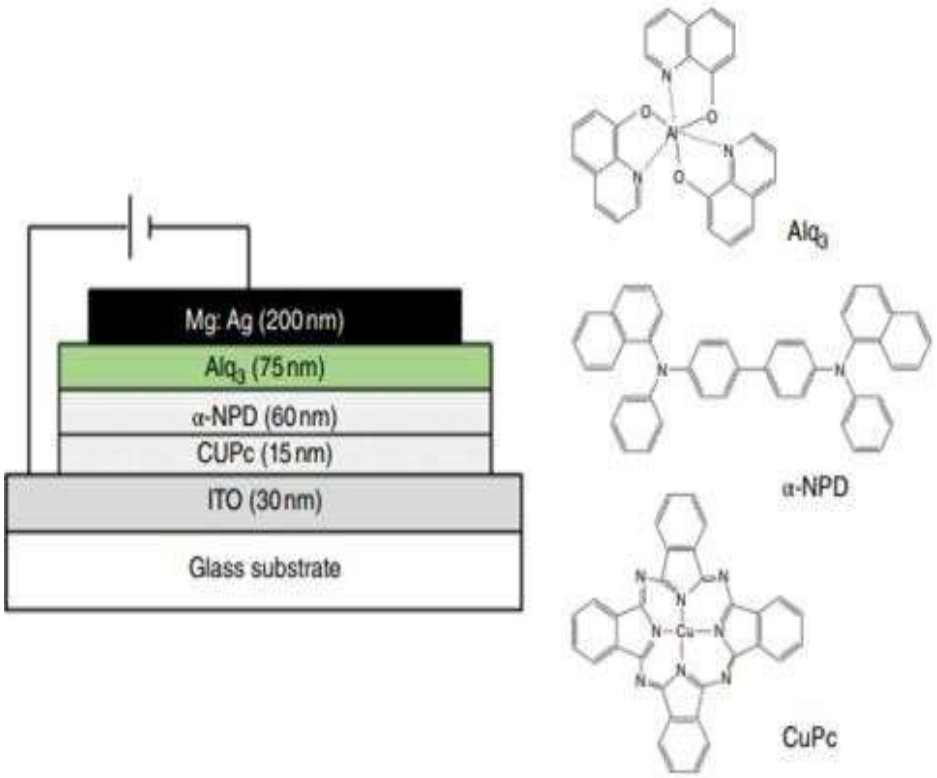

Figure 4: The Device Construction and Molecular Structures of Materials Utilized

Copper phthalocyanine (CuPc) is widely recognised as a material that's utilised for hole generation. VanSlyke et al. (year) provided a comprehensive analysis of the formation process of a copper phthalocyanine (CuPc) layer on an indium tin oxide (ITO) anode, along with the incorporation of a hole transport layer of N,N′-diphenyl-N,N′-bis(1-naphthyl)-1,10-biphenyl-4,4′-diamine (NPD) [12]. The provided graphic depicts a schematic that showcases the configuration of the equipment under investigation, together with the component compositions of the materials used in its construction. The ionisation potential of copper phthalocyanine (CuPc) is seen to be 4.7 electron volts (eV), a value that is somewhat lower than the ionisation potential of N,N'-di(naphthalen-1-yl)-N,N'-diphenylbenzidine (NPD), whose is determined to be 5.1 eV. Indium Tin Oxide (ITO) has an ionisation potential of around 4.7 electron volts (eV), indicating indicates the energy barrier separating ITO from Copper Phthalocyanine (CuPc) is somewhat smaller in comparison to the energy barrier between ITO and N,N'-Di(1-naphthyl)-N,N'-diphenylbenzidine (NPD). According to the details that are supplied in the source's publication, it is indicated that reducing the distance between the surfaces has the potential to impact the efficiency of hole injection and enhance the overall durability.Multicolor compounds with substantial chemical structures are often used as hole injection materials. The first investigation of the subject issue was conducted by Shirota et al. from Osaka University [13, 14]. The molecule often referred to as 4,4′,4″- tris(N-(3-methylphenyl)-N-phenylamino)triphenylamine (mMTDATA) is seen in Figure 2.3.Shirota et al. conducted a study that showcased the incorporation of mMTDATA into an organic light-emitting diode (OLED) framework, resulting in enhanced efficiency and extended operational lifespan. The primary objective of this study was to examine the impact of mMTDATA on the operational efficacy of an organic light-emitting diode (OLED). According to the results of a study [14], it has been noted that the OLED device, which utilises the

ITO/mMTDATA(60nm)/TPD(10nm)/Alq3 (50nm)/MgAg structure, exhibits a quantum efficiency that is approximately 30% higher and a longer operational lifespan compared to the conventional device that employs the ITO/TPD(10nm)/Alq3 (50 nm)/MgAg structure.

A specific kind of high-index liquid crystal (HIL) material often referred to as 1,4,5,8,9,11-hexaazatriphenylene-hexacarbonitrile (HAT CN) is frequently seen. This chemical architecture appears in Figure 2.3. HAT-CN is often used in commercial OLED displays since of its beneficial properties, including high mobility and excellent hole injection into the subsequent layer. Rhee et al. (year) did a research at Sunmoon University and the Korea Institute of Materials Science in South Korea to examine the effects of HATCN via a comparative comparison with other HIL materials [15].

Based on the existing body of research, many artificial oxides have been identified as potential candidates for use as hole input layers, hence enhancing the efficiency of organic light-emitting diodes (OLEDs). Molybdenum trioxide (MoO3) finds extensive use in practical applications pertaining to organic light-emitting diode (OLED) goods.

Researchers Tokito et al., which are affiliated with Toyota Central Research and Development Laboratories in Japan, explore the use of thin metal oxides, namely vanadium oxide (VOx), molybdenum oxide (MoOx), and ruthenium oxide (RuOx), as a hole injection layer [16]. namely, the researchers focus on vanadium oxide (VOx), molybdenum oxide (MoOx), and ruthenium oxide (RuOx). When compared to the ITO electrode, which is the one that is utilized the most often, the operating voltage of a device that uses metal oxides for hole injection is lower. The lowering in the energy barrier that contributes to the incorporation of holes into the hole transport layer may be responsible for the result that was seen.

Numerous metal oxides, including silicon dioxide (SiO2) [17], copper oxide (CuOx) [18], nickel oxide (NiO) [19, 20], and tungsten trioxide (WO3) [21], are examples of possible hole injection materials that have been suggested and researched.

Matsushima and Murata et al. conducted a research investigation at the Japan Advanced Institute of Science and Technology to investigate the impact of a MoO3 layer on hole injection characteristics. Scientists have made a significant finding on the interplay between the atomic structures of indium tin oxide (ITO), molybdenum trioxide (MoO3), and N,N'-di(naphthalene-1-yl)-N,N'-diphenylbenzidine (NPD) within the framework of organic light-emitting diode (OLED) development. The researchers observed that the incorporation of a 0.75nm MoO3 layer resulted in the development of an interface that exhibited ohmic hole injection. Furthermore, it has been postulated in citation [22] that the inherent current- voltage (I-V) characteristics of the circuit are governed by a space-charge-limited conduction.

An technique that may be used is the incorporation of a p-doped hole injection layer. A research was undertaken by Zhou, Leo, and their colleagues at Technische Universitat Dresden in Germany, focusing on the utilisation of a hole injection layer composed of TDATA filled with F4TCNQ [23]. Figure 2.5 illustrates the arrangement of the TDATA device and its constituent elements. The provided data illustrates that a device using OLED technology, particularly including 2% F4 TCNQ, requires an operating voltage of 3.4V in order to achieve a brightness level of 100 cd/m2. In comparison, an OLED device without F4 TCNQ needs a higher operating voltage of 9V.

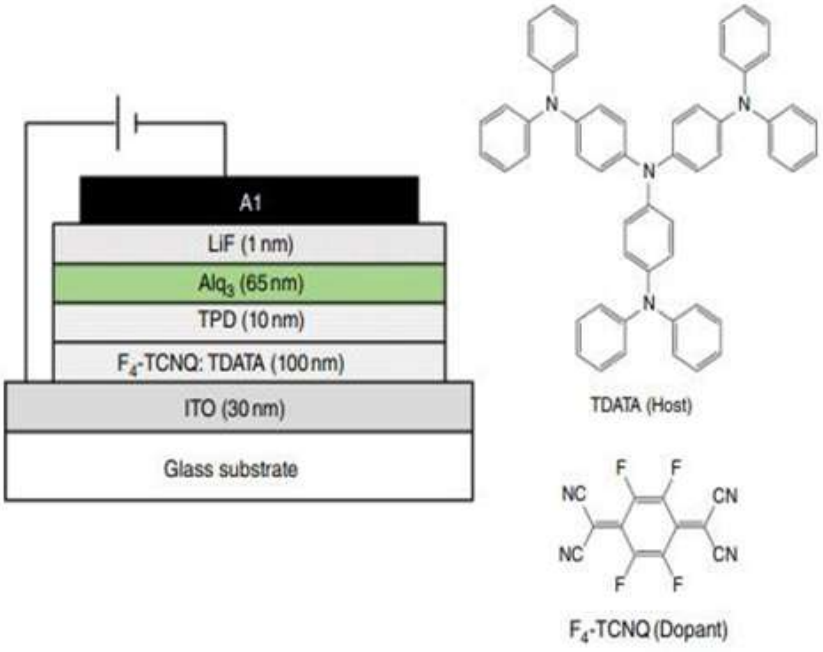

Figure 5: OLED Device Development with a Hole Injection Layer Made of TDATA Doped Alongside F4 TCNQ

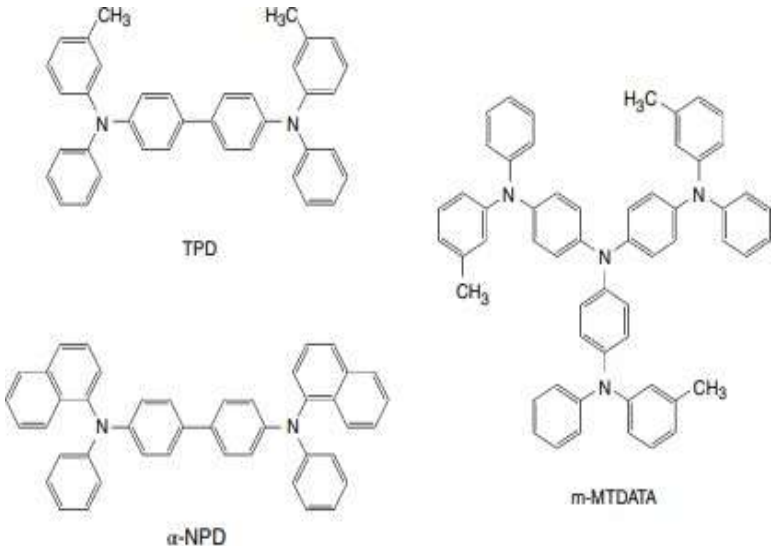

Figure 6: Conventional OLED Hole Transit Materials

2. **Hole Transport of OLED Materials:** The most significant function that hole material movement plays is to facilitate the migratory of holes in an effective manner towards the emissive layers. The aforementioned procedure is shown in detail in the [insert figure number] figure. In organic light-emitting diodes, often known as OLEDs, aromatic amino compounds are frequently utilized as the components that carry holes. The usage of N,N′-diphenyl-N,N′-bis(3-methylphenyl)-[1,1′-biphenyl]-4,4′-diamine (TPD) as a conventional hole transport substance inside the OLED device was described by Tang et al. (1987) [24]. TPD is renowned for its exceptional hole mobility, and vacuum deposition is a practical technique for fabricating an amorphous TPD film on a substrate. Nevertheless, this particular film has a tendency to undergo crystallisation when subjected to normal room

temperatures for a prolonged duration owing to its comparatively low glass transition temperature (Tg), which is around 60°C. The effectiveness of the film is significantly reduced due to changes in its structure caused by crystallisation, which in turn leads to a decrease in the effective contact area with the anode [25].

The hole transport materials that are now being considered have an elevated glass transition temperature, with special reference to 4,4′-bis[N-(1-naphthyl)-N-phenyl- amino]. Two prominent instances of such substances are biphenyl (NPD) and starburst amines.

According to a study [26], the glass transition temperature (Tg) of NPD has been documented to be around 95°C. The NPD molecule has the inherent potential to undergo oxidation, leading to the generation of the NPD+ cation. In contrast, it is possible for the NPD+ cation to undergo a reduction process, resulting in the restoration of the initial NPD molecule. In addition, it is noteworthy that the NPD++ cation, with a bivalent positive charge, has the capacity to engage in reversible oxidation and reduction reactions.

Starburst amines, namely amines 13, 14, 27, and 29, has the potential to not only occupy voids but also reposition them. The representation of a variety of starburst amines within the category is shown in Figure 4.7. The materials under consideration exhibit substantial molecular structures that impede their capacity to assume a planar shape. This phenomenon hinders the reorientation of molecules, hence impeding the crystallisation process. The persistent amorphous glassy state shown by starburst amines is an essential need in the context of organic light-emitting diode (OLED) devices. Starburst amines have been used as hole injection materials in combination with other hole transport materials, such as NPD [14].

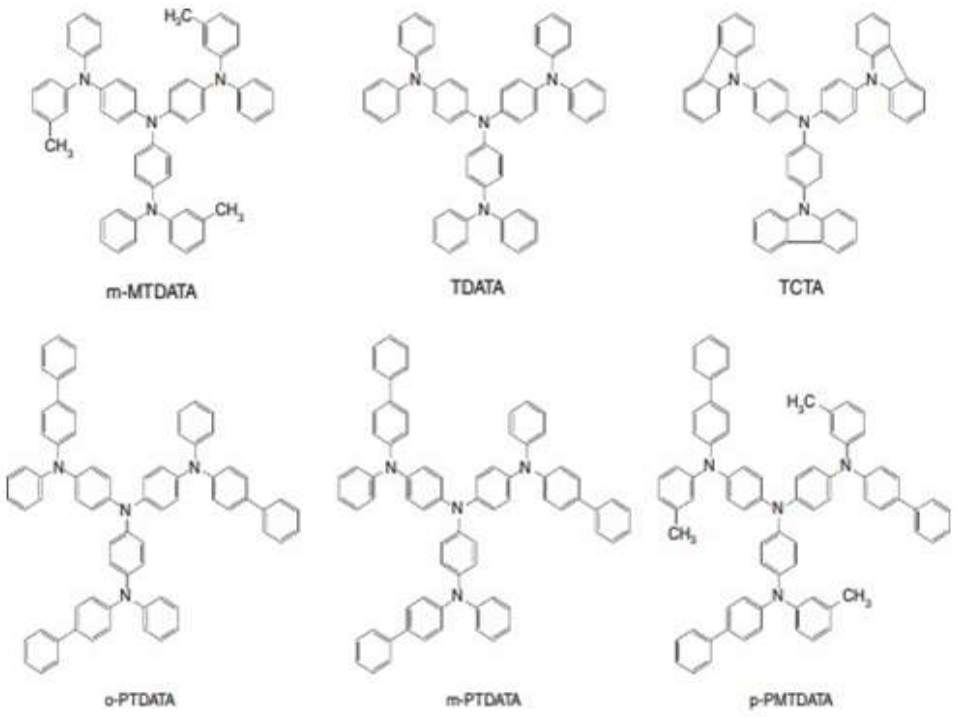

Figure 7: Illustrations of Starburst Amines for OLEDs

3. **Fluorescent Emission Layer Emitting Materials as well as Host Materials:** The principal function of materials beneath the emission layer that makes up organic light- emitting diodes (OLEDs) is to achieve accurate colour rendition & attain optimal efficiency in light emission. The physical characteristics of materials upon release, including their shine, hue, and resilience, have a substantial impact on their total efficacy.

A host substance as well as a dopant, which together make up a guest-host framework, are often found to be among the components that were used in the procedure of layer release. Figure 2.8 displays the illuminating materials together with the substrates that are compatible with them.Perylene (blue) and distyrylamine (blue) [30], coumarin (green) [31], Alq3 (green), rubrene (yellow) [32], and many additional dicyano methylene piran derivatives (red), including DCM, DCM1, and DCM2, and DCJTB [31– 33], are often used dopants for the purpose of release. Aluminium tris(8- hydroxyquinoline) (Alq3), distyrylarylene (DSA), and other compounds are widely acknowledged as host materials. Aluminium tris(8-hydroxyquinoline) (Alq3) is a luminous material that has inherent green emission and is often used as a host matrix.

In the context of guest-host systems, it is essential that the energy gap of the guest dopant be smaller than that of the host material. Generally, the range often spans from 0.5 to 5%. The effectiveness of a narrower scope may be diminished due to difficulties in sustaining attention. At now, the predominant choice for commercial OLED devices is the use of blue-emitting fluorescent OLED materials. This preference stems from the lack of availability of deep blue phosphorescent materials in the market. However, a significant proportion of green and red compounds have previously undergone a conversion into materials for phosphorescent organic light-emitting diodes (OLEDs).

Hosokawa and colleagues from Demits Kosan in Japan produced blue organic light-emitting diodes (OLEDs) using a host material based on DSA (dibenzosilole) and a dopant material consisting of amino-substituted DSA [30]. Here are few examples of DSA hosts and

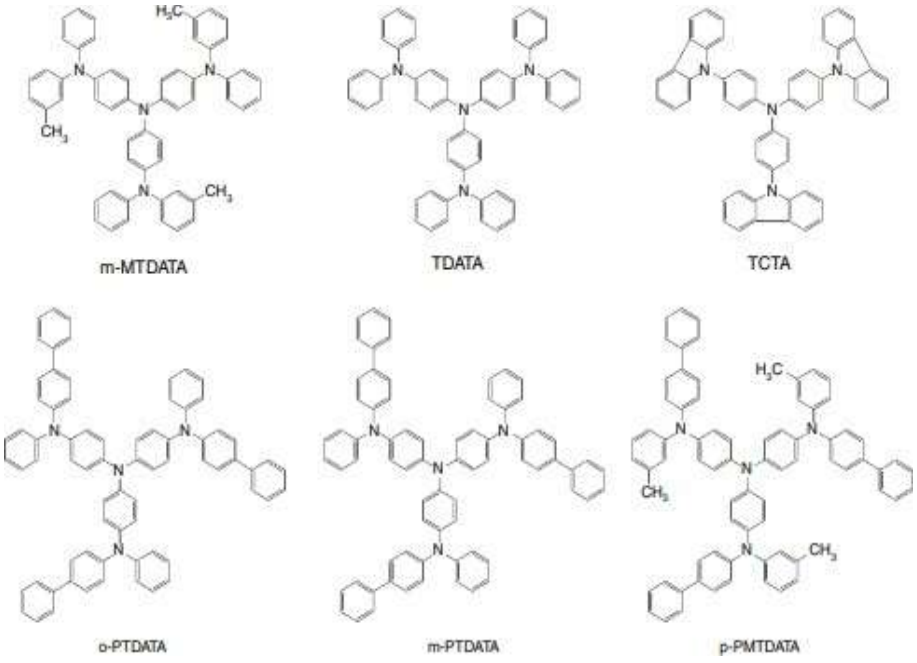

Figure 8: Fluorescent Emitting Layer Emission as Well as Host Material Illustrations

Figure 9 illustrates the incorporation of amino groups into DSA dopants. According to a study conducted in 1997, researchers reported that the use of a DSA emission layer, combined with a minimal quantity of an amino-substituted DSA dopant, resulted in an efficacy of 6 lumens per watt (lm/W) and a half-life of 20,000 hours. These findings were seen at an initial brightness level of 100 candela per square metre [34]. The first production of industrial OLED products emitting blue light included the use of these specific materials. Triplet-triplet fusion (TTF) is an intriguing phenomenon seen in luminescent organic light-emitting diode (OLED) materials exhibiting high brightness. According to Kawamura et al. from Idemitsu Kosan in Japan, the collision of triplet excitons (3A*) results in the formation of singlet excitons (1A*), as expressed by the formula provided [35].

$$3_A * + 3_A * \rightarrow {}^4/_9 .{}^1 A + {}^4/_9 .{}^1 A * + ({}^{13}/_9).{}^3 A *$$

This phenomenon is often referred to as triplet-triplet fusion (TTF), a term that accurately characterises its nature. According to Kawamura et al. (2018), a deep blue luminous organic light-emitting diode (OLED) was successfully developed by harnessing the TTF effect. The compound had a CIEy value of 0.11 and demonstrated a noteworthy EQE above 10%. Additionally, a bottom emission organic light-emitting diode (OLED) was developed, exhibiting a CIE1931 coordinate of (0.14, 0.08) and a current efficiency of 6.5 cd/A [35].

4. **The Phosphorescent Emission Layer's Emitting Materials and Host Materials:** Following the investigations of Baldo et al. from the research group led by Thompson and Forrest at Princeton University in the United States, significant progress was made in the development of phosphorescent OLED devices that exhibited favourable performance under ambient conditions [37, 38]. Consequently, there was a substantial increase in research efforts dedicated to the advancement of phosphorescent OLED technology.

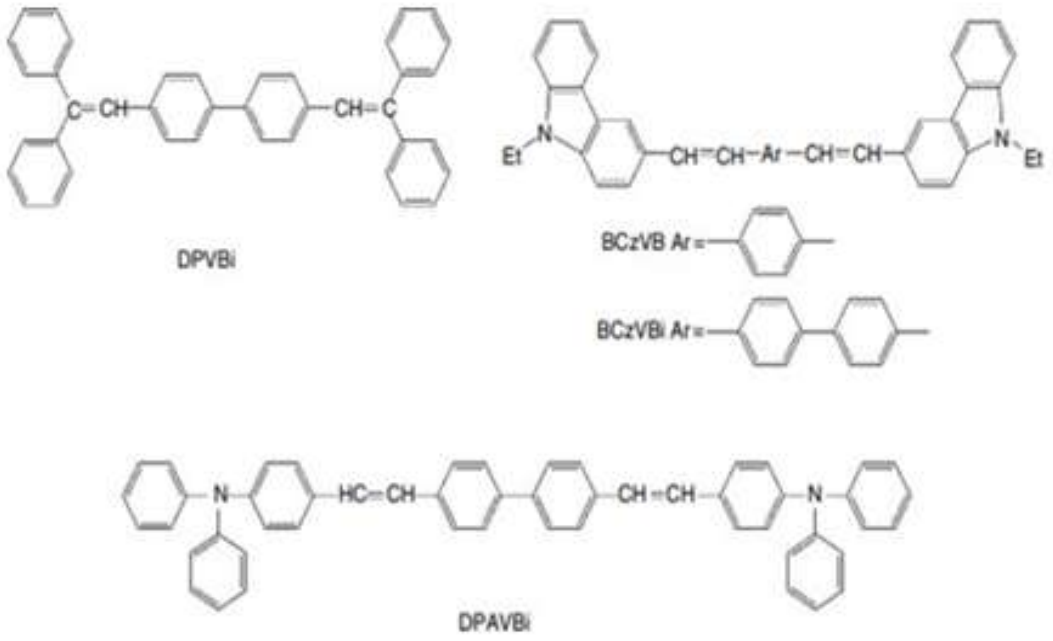

Figure 9: Molecular Structures of Blue OLED Distyrylarylene (DSA) Compounds

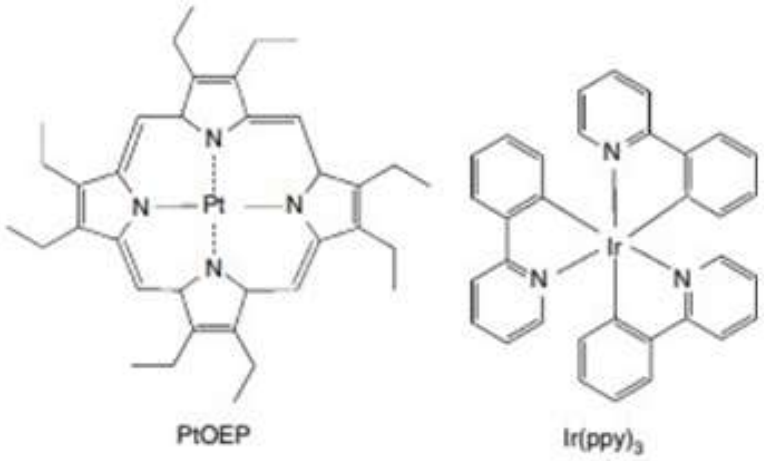

Figure 10: Structures of PEOEP And Ir(Ppy)3 at the Molecular Level.

The investigators used a phosphorescent transmitter known as 2,3,7,8,12,13,17,18-octaethyl-21H,23H-porphine platinum(II) (PtOEP) in their first investigation. Figure 2.10 illustrates the process by which the PtOEP molecules are assembled. Despite seeing phosphorescence, the researchers achieved a maximum external quantum efficiency (EQE) of just 4% [37]. In their subsequent publication, the researchers used the iridium phenylpyridine complex Ir(ppy)3 (depicted in Figure 2.10) and documented notable levels of efficacy, including an external quantum efficiency (EQE) of 8%, a current efficiency of 28cd/A, and a power efficiency of 31 lm/W [38].

The energy graph of the OLED device containing Ir(ppy)3 is shown as Figure 2.11 [38]. A relatively small amount of Ir(ppy)3 was incorporated into the CBP host matrix inside the emissive layer. The experimental trials yielded the most favourable findings when the amount of doping had been set at 6%. To restrict excitons inside the luminous area and maintain a high degree of efficiency, a narrow barrier layer of BCP was implemented between the electron transportation layer (Alq3) and the emission surface.

Investigations have also shown that the internal quantum efficiency is almost 100% [39–41].

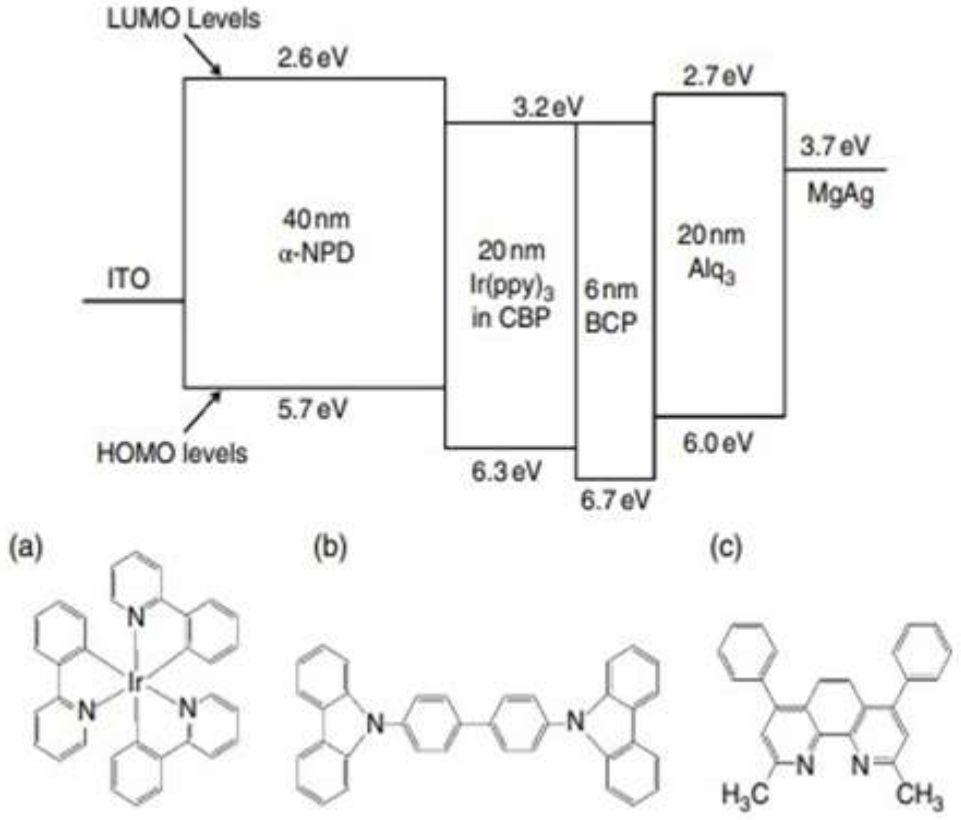

Figure 11: Illustrates the Energy Level Structure of the OLED Instrument Containing Ir(Ppy)3.Note that Ir(Ppy)3's HOMO and LUMO Levels are Unresolved the Embedded Image Depicts the Chemical Structures Of (A) Ir(Ppy)3, (B) CBP, And (C) BCP.

- **Phosphorescent-Emitting OLED Dopants are Substances:** As mentioned earlier, phosphorescent organic light-emitting diode (OLED) technologies typically include phosphorescent dopant and host material inside their emission layers. Phosphorescent organic light-emitting diodes (OLEDs) use metal clusters, which consist of metallic elements with names like iridium, platinum, ruthenium, osmium, or rhenium, to serve as emissive materials.

  According to the illustration shown in Figure 2.14, there exist two unique categories of geometrical isomers, namely face isomers and meridional isomers. The researchers from the University of Southern California (USA), Tamayo et al., conducted a study on the face and meridional isomers of several Ir-complexes [44]. They subsequently provided the following findings:

  - The surface isomer is more stable from a thermodynamic point of approach than the meridional isomer. The thermodynamic product is the face isomer, and the kinetic result is the meridional isomer. At high temperatures, it's easy to switch from the meridional isomer to the face isomer.
  - When controlling the chemical conditions, each isomer can be made in manner that renders it selective.

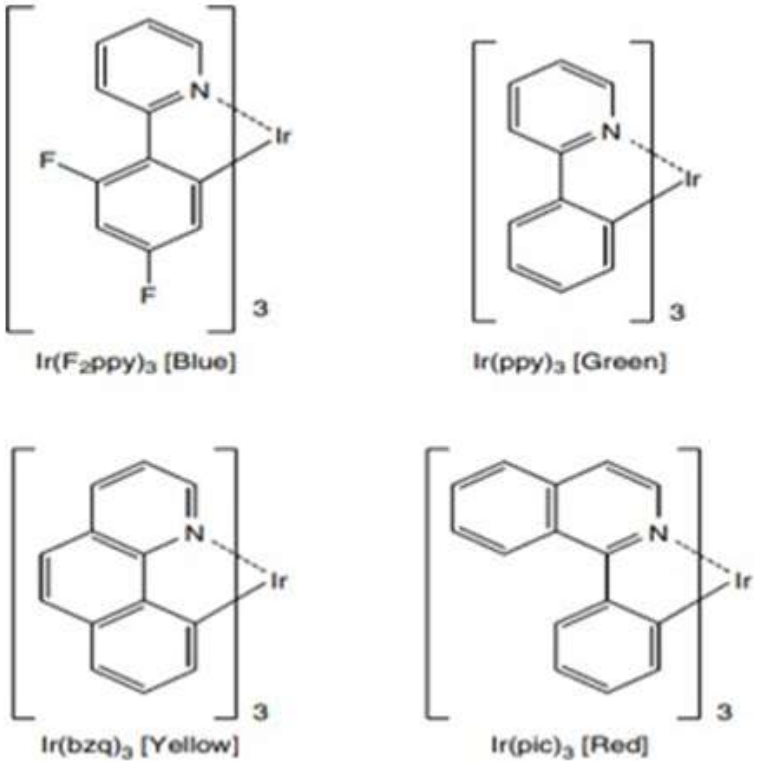

Figure 12: Trisligated Ir Phosphorescent Clusters

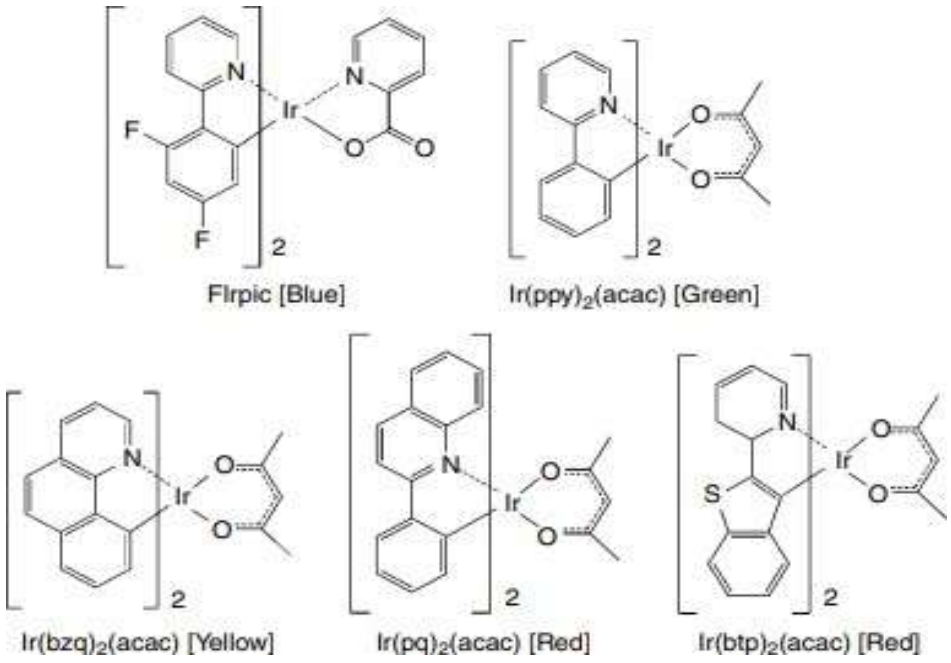

Figure 13: A Type of Phosphorescent Ir Clusters with Two Ligands

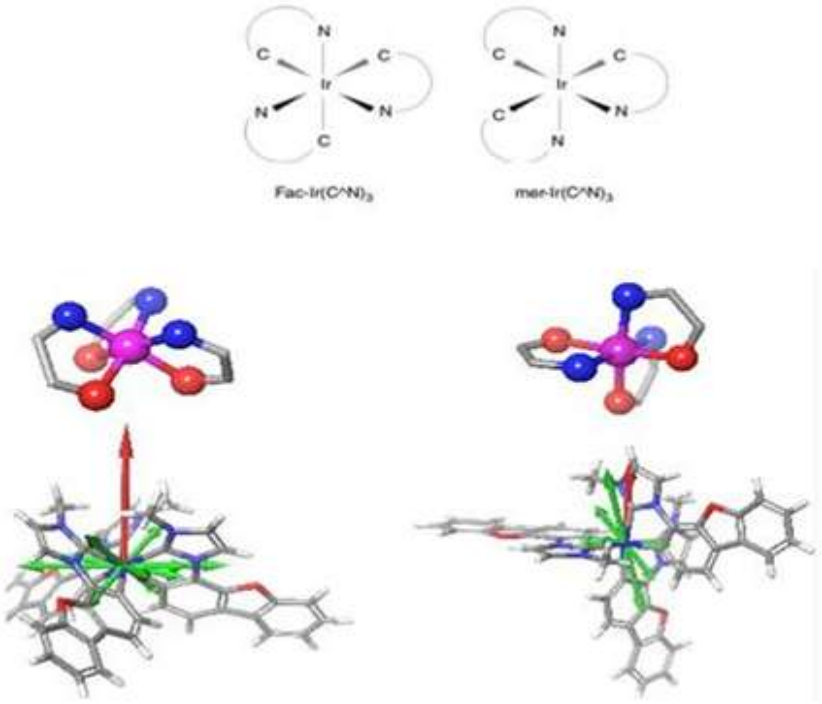

Figure 14: Ir(Ppy)3 Isomers are Compounds with A Face and A Meridional Axis

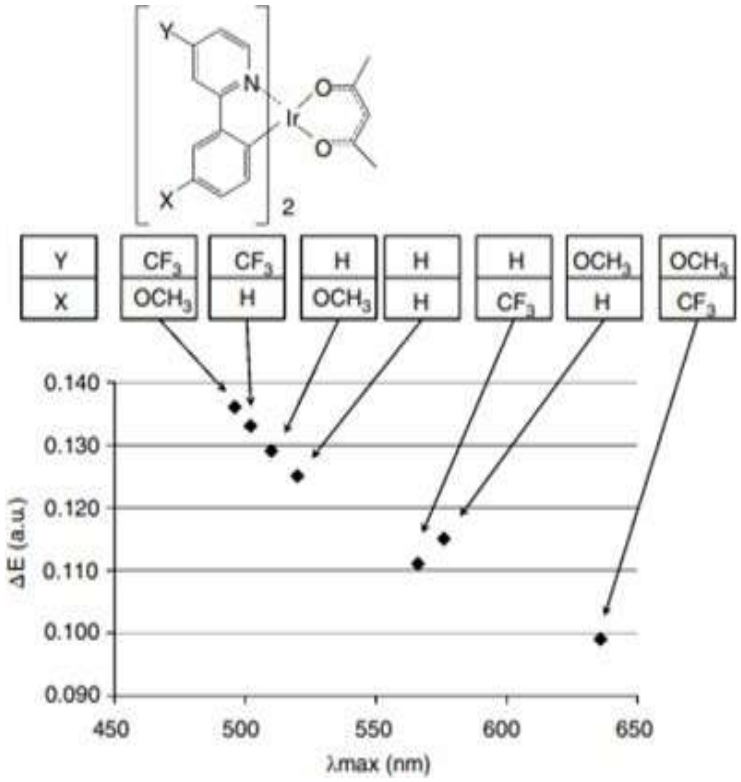

Figure 15: Demonstrates The Way Phosphorescent Ir Clusters Change The Emission Wavelength [45]. The Energy Gap Between The HOMO And LUMO States Is Given By ΔE. Λmax Is The Longest Wavelength At Which Each Phosphorescent Ir Complex Starts To Glow In The Dark.

In contrast to the face isomer, the meridional isomer has a broad emission spectrum that is shifted towards the red end of the colour spectrum.The photoluminescent atomic efficiency of the facial isomer exhibits a higher magnitude in comparison with that about its meridional isomer.

Yoshihara et al. (2021) did a research investigation at Gunma University in Japan to examine the impact of substituents on the emitted wavelength of light by phosphorescent Ir- complexes [45]. The illustration shown in Figure 2.15 portrays the resultant consequence of the given scenario. The solution comprises toluene. The photoluminescent phosphorescent emissions spectra were recorded. The investigators examined the discrepancy in energy levels between the highest occupied molecular orbital (HOMO) and the lowest unoccupied molecular orbital (LUMO), which is represented as ΔE. Previous studies have shown a strong correlation between the emission peak wavelength and the magnitude of ΔE. Regarding the vertical position, it can be seen that the CF3 group, known for its electron-withdrawing characteristics, leads to a reduction in the emission wavelength. In contrast, the OCH3 group, possessing electron-donating properties, results in a rise in the emission wavelength.

On the contrary, at the X-position, the connection undergoes inversion. In the X-position, the inclusion of the CF3 group induces an electron-withdrawing phenomenon, hence causing a rise in the emission wavelength. In contrast, the OCH3 group located at the same location demonstrates an electron-donating phenomenon, resulting in a reduction in the emission wavelength. Presently, there is seen use of red and green phosphorescent substances in several commercially available items. Nevertheless, the development of blue phosphorescent materials still faces several obstacles, notably in terms of achieving high colour purity and long-term stability. The emission characteristics of the blue phosphorescent materials FIrpic (iridium(III)bis(4,6- di- fluorophenyl)- pyridinato- N,C- 2′)picolinate) and FIr6 (iridium(III)bis(4′,6′- difluorophenylpyridinato)tetrakis(1- pyr azolyl)borate) have gained significant recognition. The compound FIrpic has a peak emission at a wavelength of 470 nm, whereas FIr6 emits light at a slightly shorter wavelength of 458 nm. It is important to acknowledge that both emission bands have a broad distribution in the green part of the electromagnetic spectrum, with a progressive shift towards the bluish-green range. Researchers are now engaged in ongoing endeavours to create blue phosphorescent devices. The collection of newly created blue phosphorescent emitters is shown in Figure 16. The study presented a series of cyclometallated carbene-iridium complexes that exhibited promising characteristics as highly efficient blue emitters, demonstrating increased photoluminescence properties [46]. The primary compound used is mertris(Ndibenzofuranyl N′methyl imidazole)iridium(III) (Ir(dbfmi)), which exhibits luminescence in the blue region of the electromagnetic spectrum with a peak wavelength of 445 nm. The blue organic light- emitting diode (OLED) using iridium (dbfmi) as the emitting material demonstrated a peak power efficiency of 35.9 lumens per watt (lm/W). By using the previously described techniques, a white organic light-emitting diode (OLED) device was effectively fabricated, demonstrating an impressive peak power efficiency of 59.9 lumens per watt (lm/W). It is important to highlight that there were no improvements made in relation to light-out coupling.

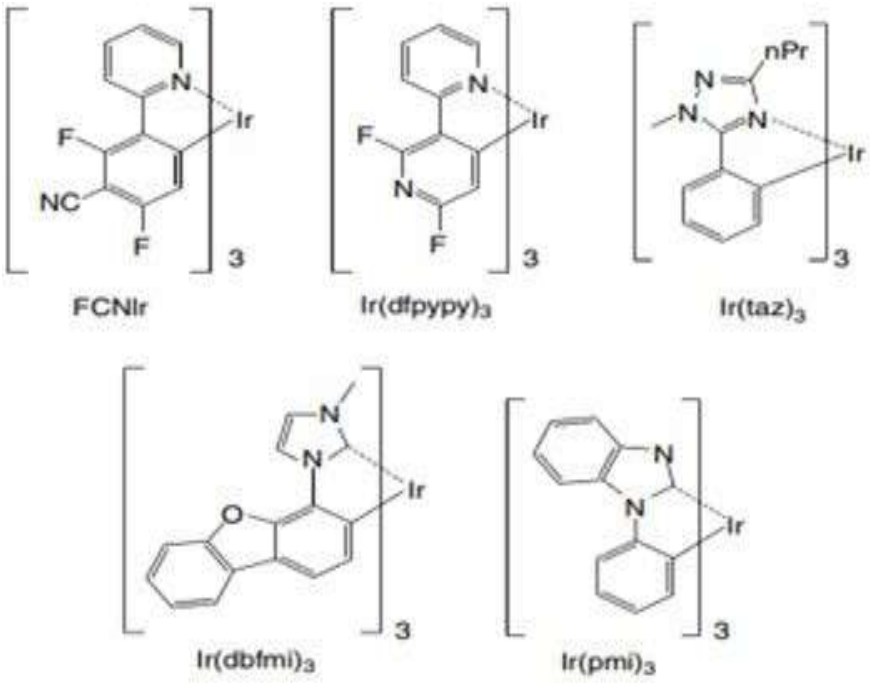

Figure 16: Various of Blue Phosphorescent Emitters

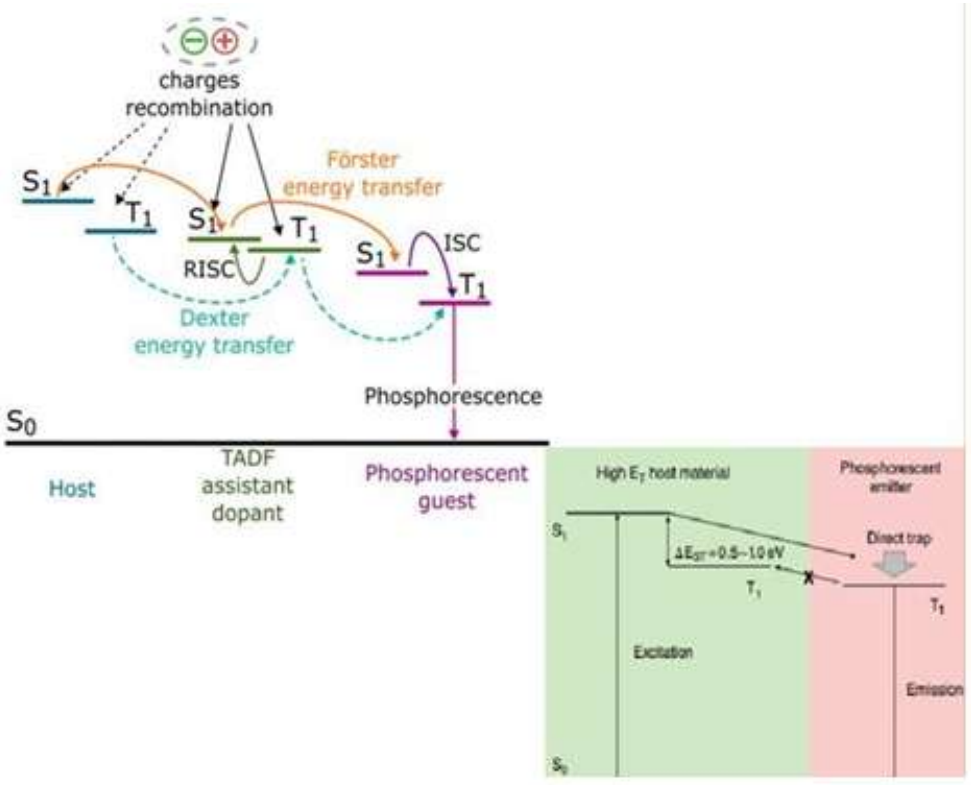

Figure 17: Is A Graphic Illustrating The Energy Transmission In Phosphorescent Oleds with a Host Material And Phosphorescent Emitter.

- **Materials which Encourage Blue Phosphorescent OLEDs:** While the development of blue phosphorescent OLED technology still encounters obstacles, the use of red and green phosphorescent OLED materials has gained significant traction across several industrial sectors. The absence of an appropriate substrate material for the bonding of the phosphorescent blue discharge layer is a contributing element to this problem. The functioning of blue phosphorescent OLEDs necessitates the use of wide energy gap organic materials or materials with high triplet excited energy levels (ET).

As seen in Figure 17, it is essential to produce organic host materials and charge transporting materials that possess substantial energy gaps. To get the intended result, it is important to possess both a limited energy difference, denoted as the S1 and T1 states, and a significant energy transfer (ET). In order to ensure the effective functioning of blue phosphorescent organic light-emitting diodes (OLEDs), it is essential that the host materials exhibit a substantial triplet energy (ET) above 2.75 electron volts (eV). Adachi et al. (Princeton University, USA) performed a research wherein they noticed that the incorporation of FIrpic doped to 4,4′-N,N-′-dicarbazole- biphenyl (CBP) in an OLED device resulted in the manifestation of blue phosphorescent emission, characterised by a peak wavelength of 470 nm. Furthermore, the device exhibited an impressively high maximum external quantum efficiency of (5.7±0.3)% and a luminous power efficiency of (6.3±0.3)lm/W, as reported in reference [42]. Based on the information provided by sources [47, 48], it has been shown that CBP and FIrpic possess triplet energies of 2.6 eV and 2.7 eV, respectively.

The deficient containment of energy may be attributed to the relatively smaller triplet energy of CBP in comparison to FIrpic. Tokito et al. (year) conducted a study at the NHK Science and Technical Research Laboratories in Japan, where they used CDBP (4,4′-bis(9-carbazolyl)-2,2′-dimethyl-biphenyl), a derivative of CBP that has a the solution of dimethyl ring [47,48]. The structure of the molecules and related energy levels of CDBP, CBP, and FIrpic are shown in Figure 2.18. The compound CDBP has a greater triplet energy of 3.0 eV in comparison to both CBP and FIrpic. The observed elevation in the triplet energy of CDBP may be ascribed to the existence of a structural distortion in the biphenyl molecule resulting from the incorporation of two methyl groups in the ortho position. The observation of a higher triplet energy for CDBP compared to FIrpic suggests the occurrence of an energetically favourable energy transfer from the triplet state of CDBP to the triplet state of FIrpic. The observed increase in efficiency may be attributed to the aforementioned mechanism for exchange of energy.

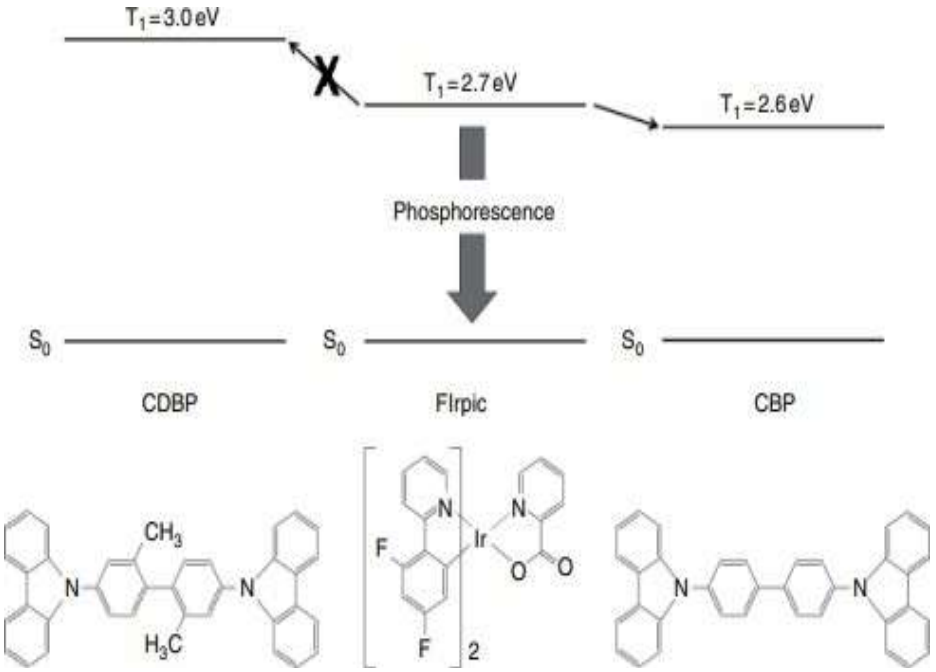

Figure 18: The exhibits the molecular structures as well as energies of CDBP, CBP, and FIrpic.

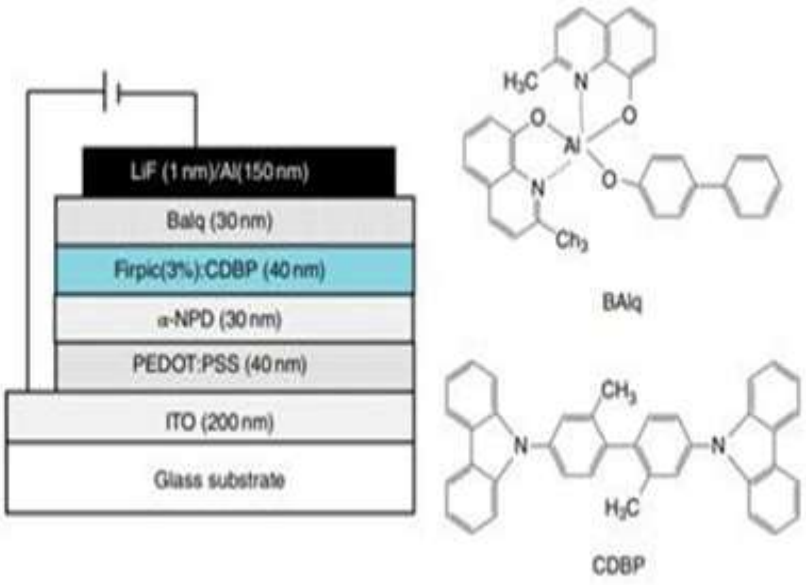

Figure 19: Shows A Blue Phosphorescent Equipment

Actually, Tokito et al. used FIrpic and CDBP to make a phosphorescent OLED technology that worked exceptionally well [47]. Figure 19 shows the construction of the device and some of the materials that are used. They said that the best external quantum efficiency they could get was 10.4%, which is the same as a current efficiency of 20.4cd/A.

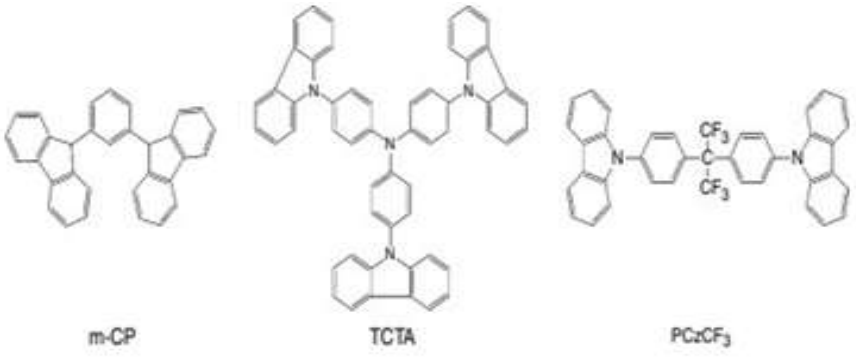

Figure 20: Is An Illustration of Newly Developed Host Materials for Blue Phosphorescent Oleds.

To far, much research has been conducted and a variety of host substances have been investigated and synthesised with the purpose of developing blue phosphorescent organic light-emitting diodes (OLEDs). Figure 2.20 illustrates many instances. A blues phosphorescent organic light-emitting diode (OLED) exhibiting high-efficiency multi-photon emission was developed by Sasabe et al. at Yamagata University in Japan. The authors reported a luminous efficacy of 90cd/A and a luminous flux efficiency of 41 lm/W [49].

5. **TADF Emission Layers, Each Layer Contains both Emitting and Host Materials:** Thermally activated delayed fluorescent (TADF) materials have considerable promise as feasible candidates for future material breakthroughs owing to their capacity to boost the performance of fluorescent substances devoid relying on the utilisation of rare metals. Figure 2.6 depicts the need for a minimum energy difference, denoted as EST, between the excited singlet state (S1) and the excited triplet state (T1) in order to facilitate thermally activated delayed fluorescence (TADF) in materials. There is a prevalent belief that a significant proportion of materials exhibiting high levels of luminescence often have an energy bandgap (Eg) falling within the range of 0.5–1.0 electron volts (eV). Based on the findings of Uoyama et al. (year), the study conducted by Adachi and colleagues at Kyushu University in Japan suggests that the optimal molecular design for achieving high luminescence in TADF materials involves a combination of two critical factors: a ΔEST value below 0.1 eV and a radiative decay rate surpassing 106 /s. Overcoming opposing non-radiative processes is necessary [50]. In light of the inherent tension between these two stipulations, it is essential to proficiently govern the convergence of the highest occupied molecular orbital (HOMO) and the lowest unoccupied molecular orbital (LUMO). Furthermore, there is a suggestion that the limitation of the molecular orientation shift between the S0 and S1 states is essential to inhibit non-radiative decay.

Uoyama et al. (year) reported the utilisation of carbazolyl dicyanobenzene (CDCB) in their study, wherein they effectively synthesised a variety of thermally activated delayed fluorescence (TADF) emitters with notable efficiency [50]. Figure 21 presents a collection of diverse illustrations of emitters using the charge-donor- charge-acceptor (CDCB) structure in the context of thermally activated delayed fluorescence (TADF). Within this particular arrangement, the carbazole constituent functions as an electron-donating entity, whilst the dicyanobenzene constituent assumes the role of an electron-accepting entity. The materials synthesised using CDCB exhibit a diverse variety of light

carbon dioxide emissions, spanning from a shade of sky-blue with a peak emission wavelength of 473 nm to a bright orange hue with a peak emission wavelength of 577 nm. The emission wavelength of light is contingent upon the electron-donating and electron-accepting properties shown by the carbazolyl group situated at the outermost region, as well as the dicyanobenzene unit situated in the central core.

Figure 22 illustrates the application of TADF materials in the fabrication of OLED devices. The green OLED device reportedly achieves an exceptionally high external quantum efficiency (EQE) of 19.3-1.5%. This EQE translates to an internal quantum efficiency (IQE) ranging from 64.3% to 96.5%, taking into account a light outcoupling efficiency of 20% to 30%.

There is now a significant amount of ongoing research and development focused on the creation of practical applications [51–53]. Figure 23 illustrates many instances.

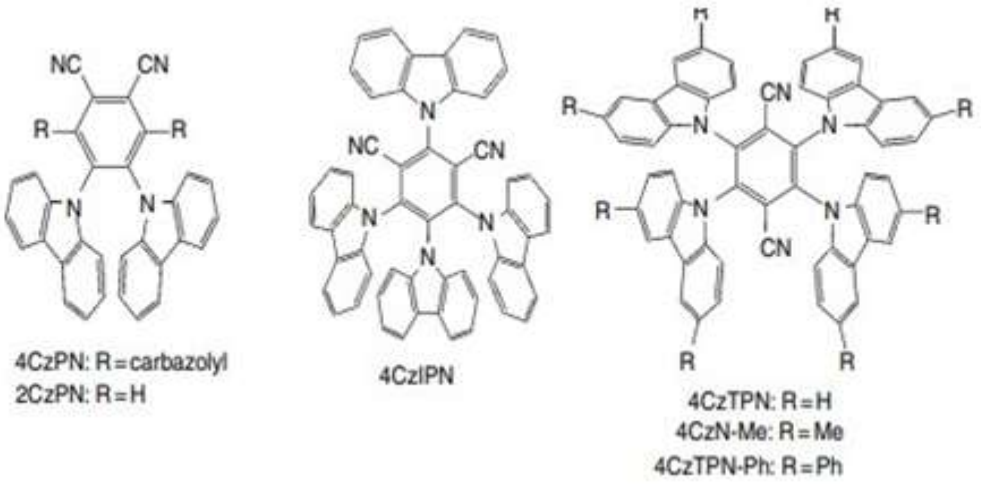

Figure 21: Illustrates Instances of TADF Emitters with CBCB Structure

6. **Electron Transport Substances:** The primary function during electron transport materials is to transfer the electrons that are introduced By traversing the several strata that release luminosity. Figure 2.24 depicts many instances of materials that have been historically used for the purpose of electron transportation. Aluminium tris(8- hydroxyquinoline) (Alq3) is a well known compound that exhibits electron mobility and emits green luminescence. The use of Alq3 in OLED devices has been extensively documented by Tang and VanSlyke [54]. This compound has been widely employed as both a luminescent material and an electron transport material.

Nevertheless, it is worth noting that organic light-emitting diode (OLEDs) produced utilising aluminium tris(8-hydroxyquinoline) (Alq3) have several limitations, namely as a consequence of their higher operating voltage and poor overall performance. The observed phenomenon may be ascribed to the intrinsic challenges faced by electrons in their movement and subsequent entry into the organic light-emitting diode (OLED) device. The available data demonstrates that several electron transport materials have been synthesised and advanced with the aim of improving the performance of organic light-emitting diodes (OLEDs). Electron-deficient aromatic hydrocarbons, including oxadiazoles, triazoles, imidazoles, pyridines, and pyrimidines, have often been used as essential components in

electron transport materials. These compounds possess a notable ability to acquire electrons from the cathode, making them valuable in numerous improvements.

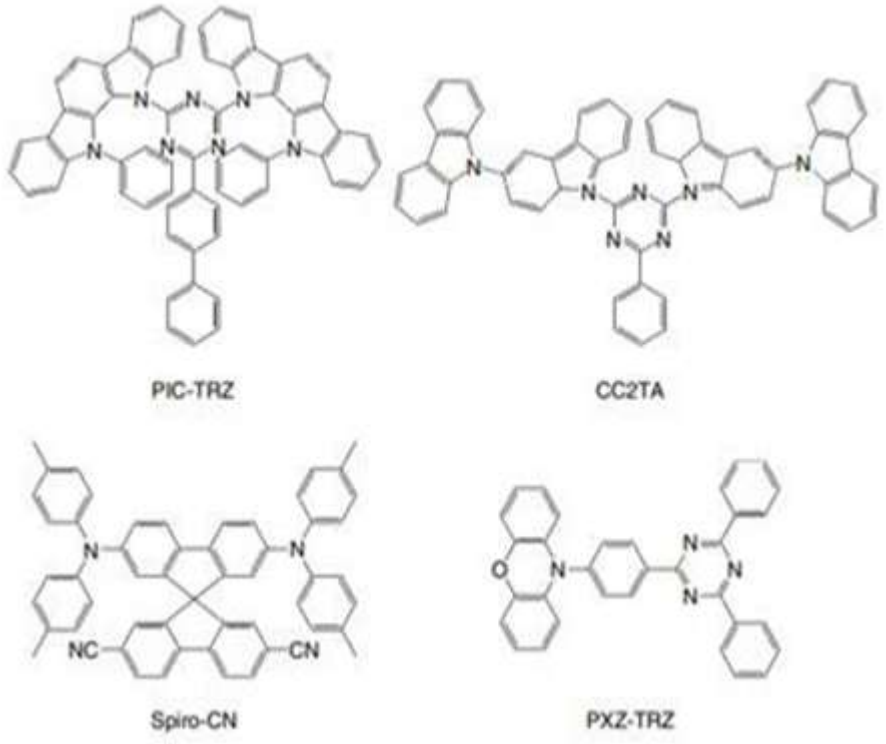

Figure 23: Examples of TADF emitters

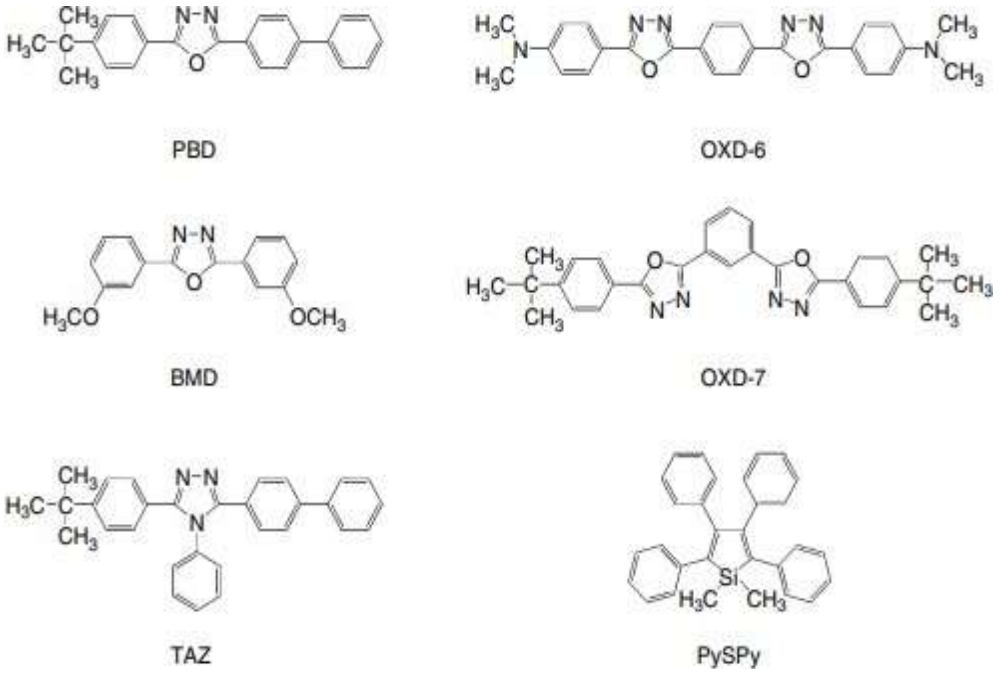

Figure 24: Electron Transport Materials with a Neoclassical Structure

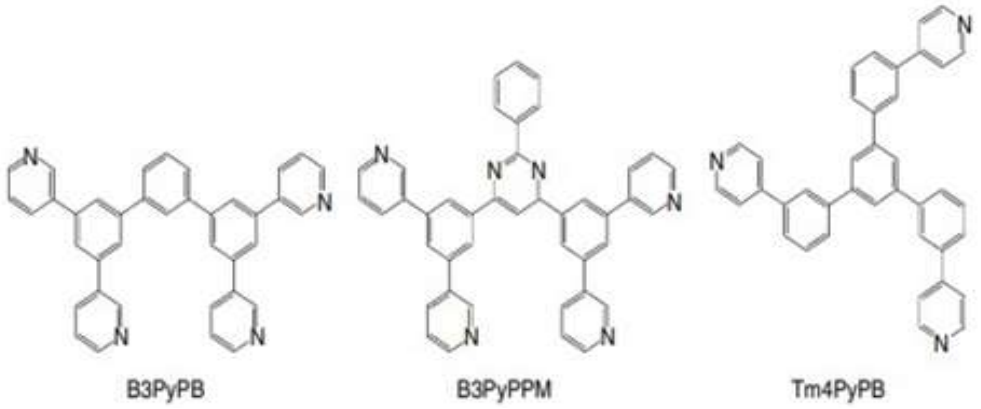

Figure 25: Identified Electron Transporting Substances

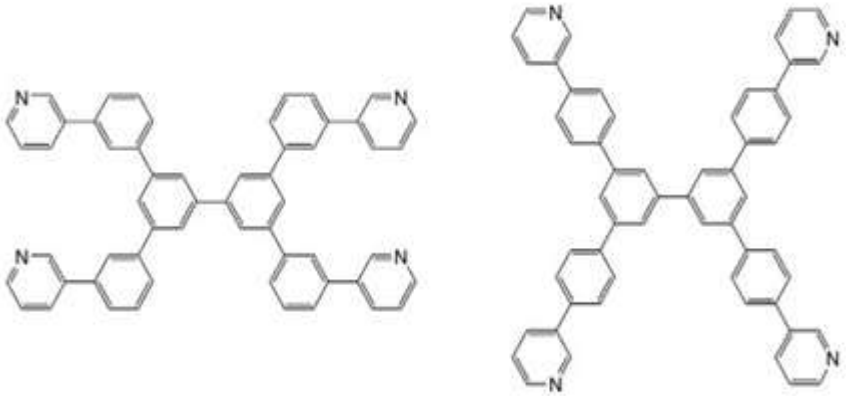

Figure 26: New Developments in Electron Transportation.

In a recent research investigation conducted by Li et al. from the Optoelectronics Industry and Technology Development Association (OITDA) and Yamagata University in Japan, novel phenanthroline derivatives (Phens) were synthesised and investigated for their potential as electron transport materials [55]. According to the statements provided by their respective firms, it has been indicated that the use of Phens results in a reduction of the turn- on voltage, hence enhancing the efficiency of Alq3.

In the context of phosphorescent OLEDs, it is essential for electron transport materials to possess a range of specific characteristics. These include a high degree of electron mobility, effective hole blocking capabilities, and an adequate triplet energy (ET) level to facilitate exciton blocking. In response to these requirements, novel materials capable of facilitating electron transport have been synthesised [56, 57]. The instances are shown in Figures 25 and 26.

7. **Material for Electron Injection as well as Cathodes:** The primary role of the cathode is to enable the transfer of electrons to an adjacent component. Hence, it's crucial to minimize the work function of the cathode. However, it's important to note that most cathode metals, such as aluminum (Al), silver (Ag), and indium tin oxide (ITO), do not have a significantly high work function. To efficiently introduce electrons into the subsequent organic layer, an additional layer called an electron injection layer (EIL) is needed.

Indeed, Electron Injection Layers (EILs) play a vital role in Organic Light- Emitting Diode (OLED) devices. This is primarily because they can effectively reduce the barrier for electron injection that exists between a cathode metal and the following organic layer, often referred to as the electron transport layer. This reduction in the injection barrier significantly lowers the operating voltage.

OLED devices often have a layer that fulfils a dual role by serving as both the electron input layer and the cathode. This specific layer is often denoted as the cathode.

Numerous investigations and advancements have been undertaken by researchers and engineers in the realm of electron injection materials, specifically focusing on the development of various kinds of electron injection layers (EILs). The group of electron injection materials known as artificial electron injection layers is well recognised. Within the realm of tiny molecule organic light-emitting diodes (OLEDs), there are noteworthy instances such as Mg:Ag [58], LiF [59–61], AlLi [62], and CsF [60]. In the field of polymer OLEDs, notable examples include the utilisation of calcium (Ca), barium (Ba), and other elements [63–67]. The research undertaken by Wakimoto et al. from Pioneer in Japan examined the effects of different combinations of alkaline metals on the operational efficiency of OLEDs [62].

The findings of the study revealed that OLED devices, when manufactured employing alkaline metal compounds, exhibited decreased power consumption during operation and exhibited improved overall performance. Jabbour et al. from the Optical Sciences Centre in the United States conducted a study to examine the influence of different cathode materials on the properties of OLEDs [60]. Based on the outcomes of their investigation, the use of an aluminium (Al) cathode exhibited a discernible elevation in driving voltage and a substantial reduction in efficiency. However, it was noted that the incorporation of magnesium (Mg), lithium fluoride/aluminum (LiF/Al), aluminium lithium fluoride (AlLiF) composite, and aluminium cesium fluoride (AlCsF) composite led to decreased driving voltages and notably improved efficiencies. The use of an ultrathin LiF/Al bilayer in organic surface-emitting diodes was investigated in the work done by Hung et al. (59). Based on the research conducted by Chen et al. (68), it was shown that the cathode layers, which consisted of stacked LiF (0.5 nm)/Al (1 nm)/Ag (20 nm), exhibited advantageous properties including a low sheet resistance of 1/sq, little optical absorption, and effective electron injection. Okamoto et al. from Sharp have effectively manufactured top-emitting organic light-emitting diodes (OLEDs) with high efficiency. This was achieved by using the micro-cavity effect, which was created by the cathode configuration of LiF (0.5nm)/Al (1nm)/Ag (20nm) [69].

At the junction between the biological cathode and the metal, it is feasible to use a very thin metal, such as magnesium (Mg) or lithium (Li), to facilitate the injection of electrons. In the research conducted by Kido et al., an experimental setup was used whereby a layer of magnesium (Mg) with a thickness of 50 nanometers or lithium (Li) with a thickness of 1 nanometer was introduced between an aluminium quinoline-3- carboxylate (Alq3) layer and a silver (Ag) cathode. This modification led to a significant augmentation in the brightness of the produced light, as reported in reference [70].

The third type comprises of organic layers that have undergone metal doping [71, 72]. In 1998, Kido et al. did a work at Yamagata University in Japan, which focused on the

incorporation of a metal-doped Alq3 layer between an Al cathode and a non-metal- doped Alq3 layer [71]. Metals with high volatility, such as lithium (Li), strontium (Sr), and samarium (Sm), are used as dopants. A device with a layer of lithium-doped aluminium quinolate (Li-doped Alq3) exhibited much increased brightness, surpassing 30,000 candela per square metre (cd/m2). In comparison, a device without the inclusion of the metal-doped Alq3 layer had a considerably lower luminance of just 3400 cd/m2. The notion was proposed that the incorporation of lithium (Li) inside the Alq3 layer would result in the formation of radical anions of Alq3, which would serve as intrinsic electron carriers. The Li-doped Alq3 layer exhibits remarkable characteristics, including a low barrier height for electron injection and outstanding electron conduction properties. The fourth group comprises metal complexes, including 8quinolinolato lithium (Liq, Fig. 2.27), which are used for electron addition [57,73–76]. The volatilization of these metal complexes may be accomplished within the temperature range of 200 to 300 °C, while their manipulation under normal atmospheric conditions is defined by convenient handling. Endo et al. (73) examined and compared two independent techniques for the deposition of metal clusters onto OLED screens in their article. The first method entails the incorporation of a metal complex stratum as an intermediate between a metal cathode and an organic stratum. An alternative methodology involves the integration of a biologically sourced material imbued with a metal complex as a supplementary stratum. A new study conducted by Kido et al. from Yamagata University has been published, focusing on the examination of lithium phenolate derivatives, namely LiBPP, LiPP, and LiQP. The relevant information may be found in Figure 27 of the article, accompanied by the associated references [57, 76].

8. **Charge-Carrier and Exciton-Blocking Substances:** Charge-carrying as well as exciton-blocking materials often play a big role in making things work better, last longer, etc. In particular, it is well known that materials that block charge carriers and excitons work well in phosphorescent OLEDs.

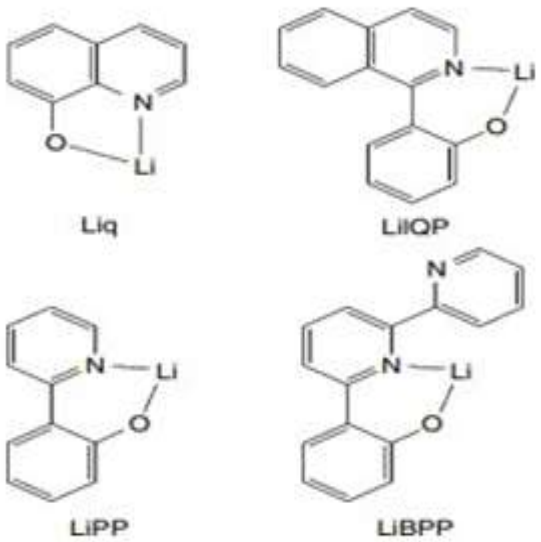

Figure 27: Illustrations of Metal Materials with Intricate Structures for EIL

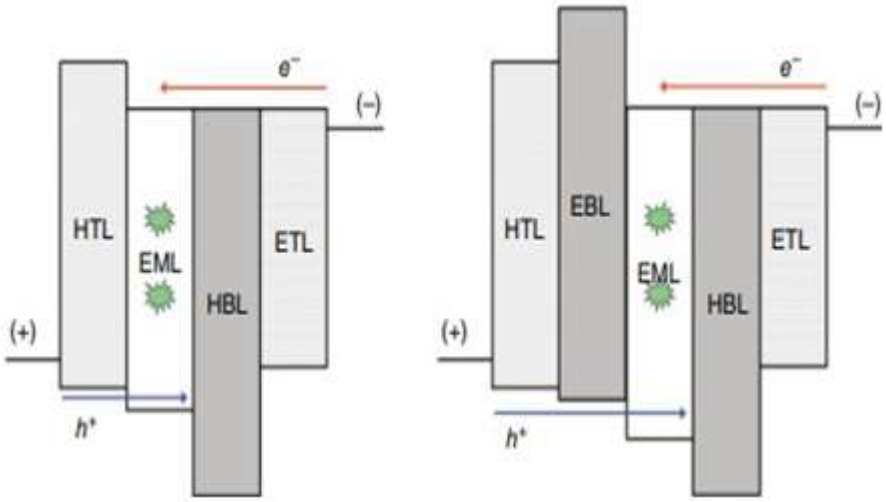

Figure 28: The Function of Charge-Carrier as well as Exciton-Blocking Substances. Excitons are Represented by Starburst Designs.

The visual representations in Figure 2.28 provide a clear illustration of the operating procedures of charge-carrier and exciton-blocking materials in terms of energy graphs. Figure 2.28(a) illustrates the positioning of a hole and exciton blocking layer (HBL) between the electron transport layer (ETL) and the emission layer (EML). The hole-blocking layer (HBL) serves the purpose of efficiently inhibiting the undesirable flow of holes and excitons into the electron transport layer (ETL). The use of OLED technology greatly boosts the efficiency of these devices. It is anticipated that the host blue light-emitting (HBL) material would possess a highest occupied molecular orbital (HOMO) level that is comparatively lower than that of the emissive layer (EML) material. In Figure 2.28(b), the schematic diagram depicts the positioning of an electron and exciton blocking layer (EBL) in the intermediate region between the hole transport layer (HTL) and the emission layer (EML). The Electron Blocking Layer (EBL) serves the purpose of preventing the undesirable leakage of electrons and excitons into the Hole Transport Layer (HTL) by changing the carrier input to the Emissive Layer (EML). This greatly improves the effectiveness of OLED devices. It is anticipated that the electron-blocking layer (EBL) has a higher energy level of the lowest unoccupied molecular orbital (LUMO) in comparison to the emissive layer (EML). In the realm of phosphorescent organic light-emitting diode (OLED) devices, it is of utmost importance for the electron-blocking layer (EBL) to have a higher energy triplet level. The primary function of this feature is to inhibit the undesirable migration of excitons into the neighbouring hole-transport layer (HTL), which is incapable of light generation. Efficient suppression of carrier recombination and exciton entrapment inside the emission layer may be achieved by the use of materials with charge carrier and exciton blocking characteristics. The compounds shown in Figure 2.29 serve as illustrative instances of high-brightness luminous (HBL) materials. One of the materials included in this group is BAlq, which is a well acknowledged compound denoted by the chemical formula aluminum(III)bis(2-methyl- 8-quinolinato)4-phenylphenolate [77–79]. Kwong et al. (year) demonstrated that the integration of a BAlq layer as a hole and exciton blocking layer resulted in a substantial improvement in the operating lifespan of phosphorescent organic light-emitting diodes (OLEDs). Another chemical that is well identified in the field is 2,9-dimethyl-4,7-diphenyl- 1,10-phenanthroline, which is sometimes denoted as bathocuproine BCP [79–82].The data is shown in Figure 1.29. Reference [79] provides the reported energies of the highest occupied molecular orbital

(HOMO) and lowest unoccupied molecular orbital (LUMO) of BCP as 6.5 eV and 3.2 eV, respectively. The hindered mobility of holes may be attributed to the existence of a very low energy level in the highest occupied molecular orbital (HOMO). The use of electron blocking materials is less widespread in contrast to hole blocking materials, primarily attributed to the significantly higher mobility of holes seen in many OLED systems as opposed to the mobility of electrons. Nevertheless, there are circumstances in which materials that exhibit electron-blocking properties might be beneficial. In many cases, these materials need a substantial level of triplet energy to effectively impede the escape of excitons into a non-emissive hole transport layer (HTL). The materials often used in electron beam lithography (EBL) include Irppz and ppz2 Ir(dpm), as seen in Figure 30.

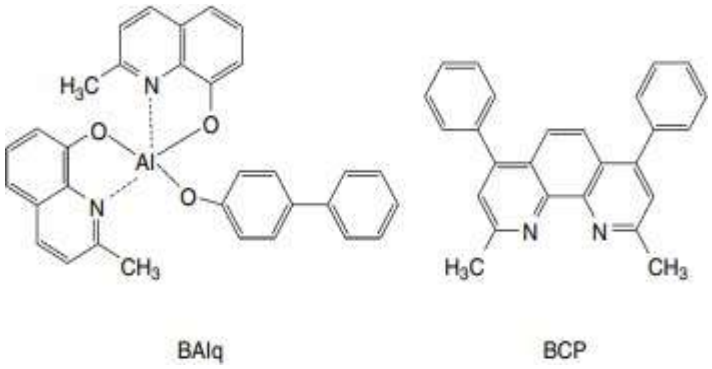

Figure 29: Typical Materials for HBL

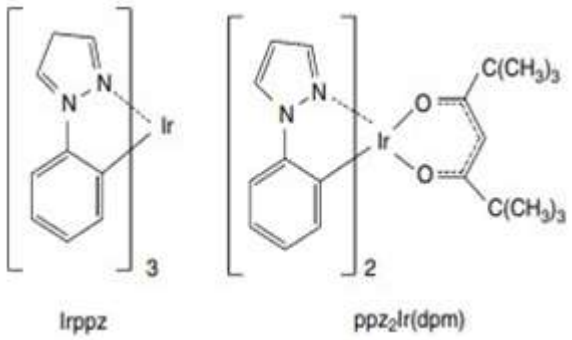

Figure 30: Illustrates the Materials Often used in Electron Beam Lithography (EBL).

9. **Materials made of N-Dope and P-Dope:** Pin OLED illumination have been shown to work well in the past when it comes to high efficiency and low power usage (23, 83–86). The structure of these p-i-n OLEDs is made up of charge blocking layers on each side and an emission layer in the middle. The wide-band gap carrier transport layers are filled with p-type and n-type materials. Conventional light-emitting diodes (LEDs) made from man-made semiconductors usually have electron and hole transport layers that are highly filled with n- and p-electron pairs. The use of tunnelling injection in this case successfully keeps the band structure constant while the LED is working. Light-emitting diodes (LEDs) that work can be made using the same ideas. An example of an OLED gadget is shown in the picture, which is called Figure 2.31.One layer is p-doped and is used for hole input and transport, and the other is n-doped and is used for electron transport. You can make organic semiconductor layers more conductive by adding electron sources for materials that move electrons or electron acceptors for materials that move holes. The voltage drop across these

layers is greatly reduced by this change. Using pin-type device designs makes it easier to get carriers from both sides into the doped transport layers. At the same time, they keep ohmic losses to a minimum in the highly conductive layers. A study by Zhou et al. at the Technische Universitat Dresden in Germany [23] talked about the p-doped hole injection layer doped with F4-TCNQ. Investigators Fujihira and Ganzorig from Japan's Tokyo Institute of Technology did a study looking into what would happen if oxidising agents like iodine, FeCl3, and SbCl5 were added to a p-doped hole transport TPD layer. The increase made both the turn-on voltage and the hole injection limit lower, according to what they found [84].It was noted that when the above oxidising chemicals were added to an ITO/TPD/Alq3/Al device, the activation voltage was less than 10V. This was different from the non-doped device, which needed a voltage of over 15V to activate. In their work [85], Ikeda et al. from the Semiconductor Energy Laboratory talked about how to use hole injection layers that are treated with molybdenum oxide (MoOx). Doped molybdenum oxide (MoOx) has also been talked about as a hole injection layer by Su et al. from I-Shou University in Taiwan [86]. In order to make a p-doped hole injection layer (HIL) in organic light-emitting diodes (OLEDs), MoOx was mixed with its p-naphthyl(phenyl)amino] triphenylamine (2- TNATA).

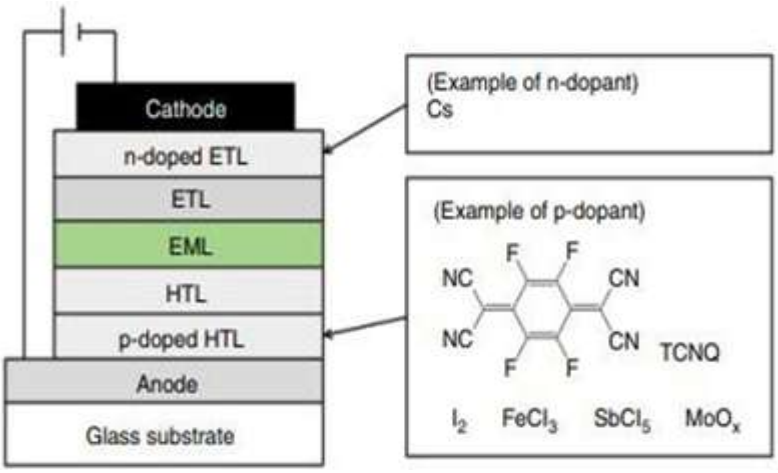

Figure 31: Exemplar of a p-i-n OLED device

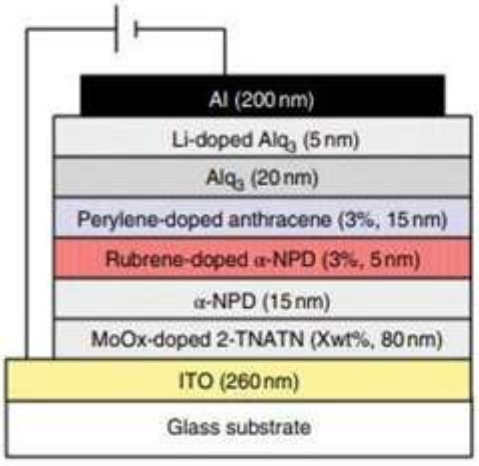

X (wt%)	Power efficiency (lm/W)
0	2.95
5	3.55
10	4.32
15	3.49
20	3.05

Figure 32: Illustrates OLED Device Structures that Employ Doped HIL and their Typical Performances.

The p-doping HIL was used in device designs, and Figure 32 shows how they usually work. The results show that adding MoOx makes the power usage better and lowers the drive voltage. They also said that the quality of life was greatly better. On the other hand, co- evaporation of BPhen with pure Cs [84] has been reported for n-doped layers.

REFERENCES

[1] H. Fukagawa, K. Watanabe, S. Tokito, Organic Electronics, 10, 798–802 (2009).
[2] A. Kawakami, E. Otsuki, M. Fujieda, H. Kita, H. Taka, H. Sato, H. Usui, Jpn. J. Appl. Phys., 47(2), 1279–1283
[3] (2008); E. Otsuki, H. Sato, A. Kawakami, H. Taka, H. Kita, H. Usui, Thin Solid Films, 518, 703 (2009).
[4] D. J. Milliron, I. G. Hill, C. Shen, A. Kahn, J. Schwartz, J. Appl. Phys., 87(1), 572–576 (2000).
[5] C. C. Wu, C. I. Wu, J. C. Sturm, A. Kahn, Appl. Phys. Lett., 70(11), 1348–1350 (1997).
[6] C. W. Tang, S. A. VanSlyke, C. H. Chan, J. Appl. Phys., 65(9), 3610–3616 (1989).
[7] L. S. Hung, L. Z. Zheng, M. G. Mason, Appl. Phys. Lett., 78(5), 673–675 (2001).
[8] C. Ganzorig, K.- J. Kwak, K. Yagi, M. Fujihira, Appl. Phys. Lett., 79(2), 272–274 (2001).
[9] I. H. Campbell, J. D. Kress, R. L. Martin, D. L. Smith, N. N. Barashkov, J. P. Ferraris, Appl. PLys. Lett., 71(24), 3528–3530 (1997).
[10] S. F. Hsu, C.- C. Lee, A. T. Hu, C. H. Chen, Current Applied Physics, 4, 663–666 (2004); S.- F. Hsu, C.- C. Lee, S.- W. Hwang, H.- H. Chen, C. H. Chen, A. T. Hu, Thin Solid Films, 478, 271–274 (2005).
[11] C. W. Chen, P. Y. Hsieh, H. H. Chiang, C. L. Lin, H. M. Wu, C. C. Wu, Appl. Phys. Lett., 83(25), 5127–5129 (2003).
[12] L.- W. Chong, T.- C. Wen, Y.- L. Lee, T.- F. Guo, Organic Electronics, 9, 515–521 (2008).
[13] S. A. VanSlyke, C. H. Chen, C. W. Tang, Appl. Phys. Lett., 69(15), 2160–2162 (1996).
[14] Y. Shirota, T. Kobata, N. Noma, Chem. Lett., 1145 (1989).
[15] Y. Shirota, Y. Kuwabara, H. Inada, T. Wakimoto, H. Nakada, Y. Yonemoto, S. Kawami and K. Imai, Appl. Phys. Lett., 65(7), 807–809 (1994).
[16] S. H. Rhee, K. B. Nam, C. S. Kim, S. Y. Ryu, ECS Solid State Lett., 3(3), R7- R10 (2014).
[17] S. Tokito, N. Noda and Y. Taga, J. Phys. D- Appl. Phys., 29, 2750–2753 (1996).
[18] Z. B. Deng, X. M. Ding, S. T. Lee, W. A. Gambling, Appl. Phys. Lett., 74(15), 2227–2229 (1999).
[19] W. Hu, M. Matsumura, K. Furukawa, K. Torimitsu, J. Phys. Chem. B, 108, 13116–13118 (2004).
[20] I- M. Chan, F. C. Hong, Thin Solid Films, 450, 304–311 (2004).
[21] H. C. Im, D. C. Choo, T. W. Kim, J. H. Kim, J. H. Seo, Y. K. Kim, Thin Solid Films, 515 , 5099–5102 (2007).
[22] J. Li, M. Yahiro, K. Ishida, H. Yamada, K. Matsushige, Synthetic Metals, 151, 141–146 (2005).
[23] T. Matsushima, Y. Kinoshita, H. Murata, Appl. Phys. Lett., 91(25), 253504 (2007); T. Matsushima, H. Murata, J. Appl. Phys., 104, 034507 (2008).
[24] X. Zhou, M. Pfeiffer, J. Blochwitz, A. Werner, A. Nollau, T. Fritz, K. Leo, Appl. Phys. Lett., 78(4), 410–412 (2001).
[25] C. W. Tang and S. A. VanSlyke, Appl. Phys. Lett., 51, 913 (1987).
[26] E. Han, L. Do, Y. Niidome and M. Fujihira, Chem. Lett., 969 (1994).
[27] S. A. VanSlyke, C. H. Chen and C. W. Tang, Appl. Phys. Lett., 69, 2160 (1996).
[28] T. Noda, Y. Shirota, Journal of Luminescence, 87–89, 1168–1170 (2000).
[29] Y. Shirota, K. Okumoto, H. Inada, Synthetic Metals, 111–112, 387–391 (2000).
[30] K. Okumoto, K. Wayaku, T. Noda, H. Kageyama, Y. Shirota, Synthetic Metals, 111–112, 473–476 (2000).72 OLED Displays and Lighting
[31] C. Hosokawa, H. Higashi, H. Nakamura, T. Kusumoto, Appl. Phys. Let., 67(26), 3853–3855 (1995);
[32] C. Hosokawa, H. Yokailin, H. Higashi, T. Kusumoto, J. Appl. Phys., 78(9), 5831–5833 (1995).
[33] J. Kido, K. Hongawa, K. Okuyama and K. Nagai, Appl. Phys. Lett., 64(7), 815–817 (1994).
[34] Y. Hamada, H. Kanno, T. Tsujioka, H. Takahashi, T. Usuki, Appl. Phys. Lett., 75(12) 1682–1684 (1999).

[35] C. W. Tang, S. A. VanSlyke, C. H. Chen, J. Appl. Phys., 65, 3610 (1989).
[36] C. Hosokawa, M. Eida, M. Matsuura, K. Fukuoka, H. Nakamura, T. Kusumoto, Synth. Met., 91, 3–7 (1997).
[37] Y. Kawamura, H. Kuma, M. Funahashi, M. Kawamura, Y. Mizuki, H. Saito, R. Naraoka, K. Nishimura, Y. Jinde, T. Iwakuma, C. Hosokawa, SID 11 Digest, 56.4 (p. 829) (2011).
[38] M. Kawamura, Y. Kawamura, Y. Mizuki, M. Funahashi, H. Kuma, C. Hosokawa, SID 10 Digest, 39.4 (p. 560) (2010).
[39] M. A. Baldo, D. F. O'Brien, Y. You, A. Shoustikov, S. Sibley, M. E. Thompson, and S. R. Forrest, Nature, 395, 151 (1998).
[40] M. A. Baldo, S. Lamansky, P. E. Burrows, M. E. Thompson, S. R. Forrest, Appl. Phys. Lett., 75, 4–6 (1999).
[41] C. Adachi, M. A. Baldo, S. R. Forrest, Appl. Phys. Lett, 77, 904–906 (2000).
[42] M. Ikai, S. Tokito, Y. Sakamoto, T. Suzuki, Y. Taga, Appl. Phys. Lett., 79, 156–158 (2001).
[43] C. Adachi, M. A. Baldo, M. E. Thompson, S. R. Forrest, J. Appl. Phys., 90(10), 5048–5051 (2001).
[44] C. Adachi, R. C. Kwong, P. Djurovich, V. Adamovich, M. A. Baldo, M. E. Thompson, S. R. Forrest, Appl. Phys. Lett., 79(13), 2082–2084 (2001).
[45] C. Adachi, M. A. Baldo, S. R. Forrest, S. Lamansky, M. E. Thompson, R. C. Kwong, Appl. Phys. Lett., 78(11), 1622–1624 (2001).
[46] A. B. Tamayo, B. D. Alleyne, P. I. Djurovich, S. Lamansky, I. Tsyba, N. N. Ho, R. Bau, M. E. Thompson, J. Am. Chem. Soc., 125, 7377–7387 (2003).
[47] T. Yoshihara, Y. Sugiyama, S. Tobita, Proc. of 6th Japanese OLED Forum, S7–2 (p. 37) (2008).
[48] H. Sasabe, J. Takamatsu, T. Motoyama, S. Watanabe, G. Wagenblast, N. Langer, O. Molt, E. Fuchs, C. Lennartz, J. Kido, Adv. Mater., 22, 5003–5007 (2010).
[49] S. Tokito, T. Iijima, Y. Suzuri, H. Kia, T. Tsuzuki, F. Sato, Appl. Phys. Lett., 83(3), 569–571 (2003);; S. Tokito, T. Tsuzuki, F. Sato, T. Iijima, Current Appl. Phys., 5, 331–336 (2005).
[50] I. Tanaka, Y. Tabata, S. Tokito, Chem. Phys. Lett., 400, 86–89 (2004).
[51] H. Sasabe, K. Minamoto, Y.- J. Pu, M. Hirasawa, J. Kido, Organic Electronics, 13, 2615–2619 (2012).
[52] H. Uoyama, K. Goushi, K. Shizu, H. Nomura, C. Adachi, Nature, 492, 234 (2012).
[53] A. Endo, K. Sato, K. Yoshimura, T. Kai, A. Kawada, H. Miyazaki, and C. Adachi, Appl. Phys. Lett., 98,
[54] 083302 (2011).
[55] Q. Zhang, J. Li, K. Shizu, S. Huang, S. Hirata, H. Miyazaki, C. Adachi, J. Am. Chem. Soc., 134, 14706–14709 (2012); bH. Tanaka, K. Shizu, H. Miyazaki, C. Adachi, Chem. Commun., 48, 11392–11394 (2012).
[56] C. Adachi, Jpn. J. Appl. Phys., 53, 060101 (2014).
[57] C. W. Tang and S. A. VanSlyke, Appl. Phys. Lett., 51, 913 (1987).
[58] Y.- J. Li, H. Sasabe, S.- J. Su, D. Takana, T. Takeda, Y.- J. Pu, J. Kido, Chem. Lett., 38(7), 712–713 (2009).
[59] H. Sasabe, J. Kido, Chem. Mater., 23, 621–630 (2011).
[60] H. Sasabe, J. Kido, Eur. J. Org. Chem., 7653–7663 (2013).
[61] C. W. Tang and S. A. VanSlyke, Appl. Phys. Lett., 51, 913–915 (1987).
[62] L. S. Hung, C. W. Tang, M. G. Mason, Appl. Phys. Lett., 70(2), 152–154 (1997).; L. S. Hung, C. W. Tang, M. G. Mason, P. Raychaudhuri, J. Madathil, Appl. Phys. Lett., 78(4), 544–546 (2001);M. G. Mason, C. W. Tang, L.- S. Hung, P. Raychaudhuri, J. Madathil, L. Yan, Q. T. Le, Y. Gao, S.- T. Lee, L. S. Liao, L. F. Cheng, W. R. Salaneck, D. A. dos Santos, J. L. Bredas, J. Appl. Phys., 89(5), 2756–2765 (2001).
[63] G. E. Jabbour, B. Kippelen, N. R. Armstrong, N. Peyghambarian, Appl. Phys. Lett., 73(9), 1185–1187 (1998).
[64] S. E. Shaheen, G. E. Jabbour, M. M. Morrell, Y. Kawabe, B. Kippelen, N. Peyghambarian, M.- F. Nabor, R. Schalaf, E. A. Mash, N. R. Armstrong, J. Appl. Phys., 84(4), 2324–2327 (1998).
[65] T. Wakimoto, Y. Fukuda, K. Nagayama, A. Yokoi, H. Nakada, M. Tsuchida, IEEE Transitions on Electron Devices, 44(8), 1245–1248 (1997).
[66] A. R. Brown, D. D. C. Bradley, J. H. Burroughes, R. H. Friend, N. C. Greenham, P. L. Burn, A. B. Holmes, A. Kraft, Appl. Phys. Lett., 62(23), 2793–2795 (1992).

[67] I. D. Parker, J. Appl. Phys., 75(3), 1656–1666 (1994).
[68] R. H. Friend, R. W. Gymer, A. B. Holmes, J. H. Burroughes, R. N. Marks, C. Taliani, D. D. C. Bradley,
[69] D. A. Dos Santos, J. L. Bredas, M. Lögdlung, W. R. Salaneck, Nature, 397, 121–128 (1999).
[70] Y. Cao, G. Yu, I. D. Parker, A. Heeger, J. Appl. Phys., 88(6), 3618–3623 (2000).
[71] T. M. Brown, R. H. Friend, I. S. Millard, D. L. Lacey, T. Butler, J. H. Burroughes, F. Cacialli, J. Appl. Phys., 93(10), 6159–6172 (2003).OLED Materials 73
[72] C. W. Chen, P. Y. Hsieh, H. H. Chiang, C. L. Lin, H. M. Wu, C. C. Wu, Appl. Phys. Lett., 83(25), 5127–5129 (2003).
[73] K. Okamoto, Y. Fujita, Y. Ohnishi, S. Kawato, M. Koden, Proc. of 7th Japanese OLED Forum, S9- 2 (2008).
[74] J. Kido, K. Nagai, Y. Okamoto, IEEE Transactions on Electron Devices, 40(7), 1342–1344 (1993).
[75] J. Kido, T. Matsumoto, Appl. Phys. Lett., 73, 2866–2868 (1998).
[76] K. Walzer, B. Maennig, M. Pfeiffer, K. Leo, Chem. Rev., 107, 1233–1271 (2007).
[77] J. Endo, J. Kido, T. Matsumoto, Ext. Abst. (59th Autumn Meet. 1998); Jpn. Soc. Appl. Phys., 16a- YH- 10 (p. 1086) (1998).
[78] J. Endo, T. Matsumoto, J. Kido, Jpn. J. Appl. Phys, 41, L800–L803 (2002).
[79] C. Schmitz, H.- W. Schmidt, M. Thelakkat, Chem. Mater., 12, 3012–3019 (2000).
[80] Y.- J. Pu, M. Miyamoto, K. Nakayama, T. Oyama, M. Yokoyama, J. Kido, Org. Electron, 10, 228 (2009).
[81] C. Adachi, R. C. Kwong, P. Djurovich, V. Adamovich, M. A. Baldo, M. E. Thompson, S. R. Forrest, Appl. Phys. Lett., 79(13), 2082–2084 (2001).
[82] R. C. Kwong, M. R. Nugent, L. M. Michalski, T. Ngo, K. Rajan, Y.- J. Tung, M. S. Weaver, T. X. Xhou,
[83] M. Hack, M. E. Thompson, S. R. Forrest, J. J. Brown, Appl. Phys. Lett., 81(1), 162–164 (2002).
[84] V. I. Adamovich, S. R. Cordero, P. I. Djurovich, A. Tamayo, M. E. Thompson, B. W. D'Andrade, S. R. Forrest, Organic Electronics, 4, 77–87 (2003).
[85] M. B. Khalifa, D. Vaufrey, J. Tardy, Organic Electronics, 5, 187–198 (2004).
[86] M. A. Baldo, S. Lamansky, P. E. Burrows, M. E. Thompson, S. R. Forrest, SR, Appl. Phys. Lett., 75(1), 4–6 (1999).
[87] C. Adachi, M. A. Baldo, S. R. Forrest, S. Lamansky, M. E. Thompson, R. C. Kwong, Appl. Phys. Lett., 78(11), 1622–1624 (2001).
[88] M. Fujihira, C. Ganzorig, Materials Science and Engineering, B85, 203–208 (2001).
[89] D. Gebeyehu, K. Walzer, G. He, M. Pfeiffer, K. Leo, J. Brandt, A. Gerhard, P. Stößel, H. Vestweber, Synthetic Metals, 148, 205–211 (2005).

